Department of Socio-Cultural Environmental Studies Graduate
School of Frontier Sciences
The University of Tokyo

2024

Master's Thesis

Spatiotemporal Distribution of Refractory Organic Matter in Tokyo Bay Using Fluorescence Properties and Degradation Experiment

(蛍光特性と分解実験を用いた

東京湾における難分解性有機物の時空間分布)

Submitted on July 12, 2024

Supervisor: Professor SASAKI Jun
Co-supervisor: Associate Professor KAZAMA Shinobu

GUO Shiyue
郭 诗岳

Contents

List of Figures

List of Tables

List of abbreviations

Dissolved organic carbon (DOC)

Labile DOC (LDOC)

Refractory DOC (RDOC)

Total organic carbon (TOC)

Sewage treatment plants (STPs)

Fluorescent dissolved organic matter (FDOM)

Excitation-emission matrices (EEMs)

Refractory organic matter (ROM)

Colored Dissolved Organic Matter (CDOM)

Dissolved inorganic carbon (DIC)

Edogawa River(Edo)

Arakawa River(AK)

Chlorophyll-a(Chl-a)

ACKNOWLEDGMENTS

Completing this research over the past two years has been a challenging endeavor. While I admit this study has some limitations, I am confident I have given it my all. I experienced confusion and frustration during this period, but I also learned how to become a persuasive scientist. The qualities I acquired during these two years of scientific research will benefit me for a lifetime.

First and foremost, I am deeply grateful to Professor Sasaki for his scientific guidance. He valued our research interests and respected our choices. From him, I learned that the essence of science lies in originality. During times of difficulty, he generously provided research funding, allowing our work to proceed smoothly. His insightful suggestions during our group meetings always gave me new perspectives and renewed motivation for learning.

I am also very thankful to Professor Hiroyasu Satoh. His classes were engaging and lively, and I particularly enjoyed our outdoor sessions in the park, which offered a completely different experience from the classroom settings in China. I am also grateful to Professor Satoh's lab for supporting my experiments, such as providing Milli-Q water.

My heartfelt thanks go to my co-supervisor, Professor Kazama. She provided numerous research suggestions and guided me on how to make my work more understandable to others. Her optimism, kindness, and warmth are inspiring. She is a strong and compassionate female scientist, the kind of person who leaves a lasting impression. From my very first seminar with her, I knew she was a teacher I would greatly admire.

I want to thank Dr. Nakamura Wataru, who was always there to answer my research questions. Whenever I felt lost, he would provide new insights. We went on two sea sampling trips together, and despite the extensive preparations and exhausting post-sampling experiments, his enthusiasm never waned. His support was crucial to my research's smooth completion; he was my guiding star in the scientific journey.

I am also grateful to everyone in our research group. Senior Wang Jie provided immense help during field investigations and experiments, teaching me both laboratory techniques and field sampling methods. Tutor Sun Jing offered considerable assistance in my daily life after I arrived in Japan. Senior Wang Yichong helped me submit essential school documents. Dr. Chen Jundong gave me long-term advice and guidance. Senior Endo taught me how to use various instruments. Senior Shao Xinlei assisted me with various Japanese-related issues in the lab. Cheng Jingwen, Yang Hanqing, and Liu Yuxuan accompanied me during field sampling. I am also thankful for the warm conversations with my friends from Myanmar, Kyaw, and my junior from the Philippines, Reign. I want to express my sincere gratitude to Dengtianan for his tremendous help during my busy final semester.

In Japan, I received significant support from many individuals. My best friend, Kou Yiqun, chose to accompany me in Japan when she learned that I couldn't return home for the New Year due to my experiments. Zheng Meizhen took care of me when I was injured. GY and Liu Yiqing traveled from

Korea to bring me supplies. Feng Haoran and Deng Xintan consistently cheered me up when I was stressed out with my thesis writing.

I want to express my deepest gratitude to my boyfriend, Wang Huidong, for his unwavering support and companionship from China to Japan. He has been a silent supporter in my life and studies, and I look forward to our long journey together.

Finally, I am grateful to my parents, Guo Guilin and Zheng Haixiang. They have always been my most robust support, providing psychological and financial backing to help me complete my master's degree. Their unwavering support gave me the courage to pursue my studies in a foreign land, fearlessly forging my future and exploring my path.

Last but not least, I want to thank myself. Despite my shortcomings, I persevered, step by step. I am grateful for the countless days and nights spent in the lab, studying in front of the computer, never giving up. Thanks to the determined and hardworking version of me who made it through.

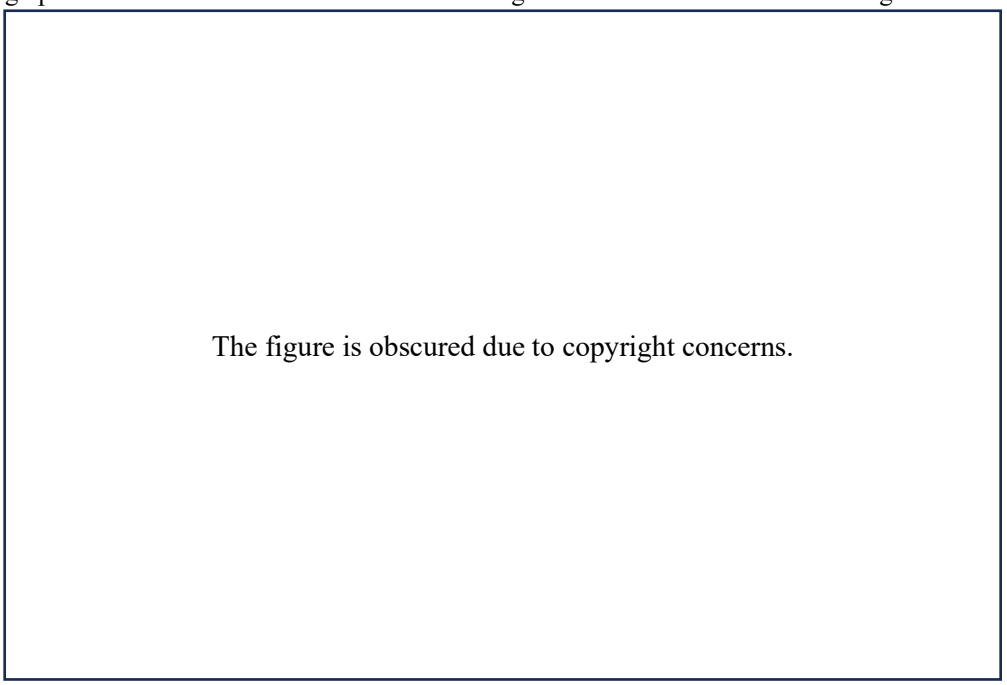

Abstract

The spatiotemporal distribution of refractory organic matter (ROM) in Tokyo Bay is essential for understanding the bay's carbon dynamics and the impact of anthropogenic activities. This study investigates the concentration and behaviors of dissolved organic carbon (DOC) and its fractions, labile DOC (LDOC) and refractory DOC (RDOC), in Tokyo Bay, leveraging fluorescence properties and degradation experiments to elucidate RDOC dynamics in this highly urbanized coastal environment.

Field surveys were conducted, and water samples were collected from the lower reaches of the Arakawa and Edo Rivers and various points within Tokyo Bay. These samples were analyzed using fluorescence EEMs and total organic carbon (TOC) measurements to quantify DOC concentrations and characterize the organic matter. We employed a 150-day degradation experiment to differentiate between LDOC and RDOC, examining the influence of filter pore sizes and incubation containers on RDOC measurements.

The results show significant spatial and temporal variations in DOC concentrations influenced by seasonal changes, as well as effluents from sewage treatment plants (STPs). High DOC concentrations were observed in the northern parts of Tokyo Bay, attributed to the freshwater inputs rich in organic matter from the rivers. RDOC concentrations remained relatively stable over the degradation period, indicating its persistence in the environment, while LDOC was rapidly consumed by microbial activity.

The fluorescence analysis identified six distinct components of fluorescent dissolved organic matter (FDOM), revealing contributions from both terrestrial and microbial sources. The study highlighted the complex interactions between different sources of organic matter and the processes governing their transformation and persistence in Tokyo Bay.

Our findings underscore the importance of understanding DOC dynamics for effective coastal management. Analyzing RDOC and LDOC removal efficiencies in sewage treatment processes provides insights into current practices' effectiveness and highlights areas for improvement. The study also emphasizes the need for standardized methodologies in DOC reactivity research to ensure data reliability and comparability.

The extensive sampling strategy across different seasons and weather events allowed for a comprehensive assessment of the temporal variability in carbon dynamics. The impact of extreme weather events, such as typhoons, on DOC concentrations was particularly notable, with significant increases in DOC levels following these events. This underscores the influence of climatic factors on the transport and transformation of organic matter in coastal ecosystems.

This research contributes to a deeper understanding of the behavior and fate of organic carbon in urban coastal settings. It provides valuable data for developing strategies to manage organic carbon inputs and mitigate the impact of human activities on coastal environments. The findings also highlight the potential of RDOC in long-term carbon sequestration, offering insights into its role in the global carbon cycle.

Keywords: Dissolved Organic Carbon (DOC), Labile DOC, Refractory DOC, Tokyo Bay

1. Introduction

1.1. Background

Dissolved organic matter (DOM) refers to various carbon-containing compounds that dissolve in water, originating from biological and geological sources and exhibiting a wide range of chemical reactivities [1]. DOC is critical in coastal areas such as Tokyo Bay, affecting overall carbon dynamics. The DOC pool is the largest organic carbon reservoir in the ocean, with an estimated 662 petagrams of carbon, comparable to the amount of carbon dioxide in the atmosphere [2]. In the 1970s, Ogura identified two components of DOC in Tokyo Bay: LDOC and RDOC. LDOC, more readily consumed by microorganisms, consists of easily decomposable organic compounds like simple sugars and amino acids, often derived from primary production within coastal ecosystems. In contrast, RDOC is more resistant to microbial degradation, persisting in the environment for extended periods and typically originating from terrestrial sources with complex molecular structures such as humic and fulvic acids [3].

Blue carbon refers to the organic carbon sequestered and stored by oceans and coastal ecosystems, particularly in vegetated areas like seagrass meadows, mangrove forests, and tidal marshes [4]. This concept was initially coined to highlight the significant contribution of these ecosystems to global carbon sequestration, and it has gained attention for its potential to mitigate climate change while offering co-benefits like coastal protection and fisheries enhancement [5][6]. Traditional blue carbon studies have examined carbon isolated from the atmosphere and sequestered in marine soils over 100 to 1000 years. Recently, however, the definition of blue carbon has expanded to include DOC that enters the ocean through rivers and coastal ecosystems, remaining in the marine environment without significant decomposition [7]. This inclusion is important because the decomposition of LDOC into dissolved inorganic carbon (DIC), including CO2, leads to concerns about CO2 re-emission to the atmosphere due to the equilibrium between water and air.

DOC is pivotal in aquatic ecosystems, influencing the global carbon cycle, water quality, light penetration, and microbial food webs. Fluorescent dissolved organic matter (FDOM) enables the characterization of DOC through its unique fluorescence under specific light wavelengths, offering insights into DOC origins, transformations, and ecological impacts [8]. FDOM's types trace back to various sources, including terrestrial vegetation, microbial activities, and anthropogenic inputs, each with specific environmental implications. Refractory organic matter (ROM), known for its resistance to microbial degradation, is crucial in carbon sequestration and nutrient cycling within aquatic environments [9]. Urban coastal areas such as Tokyo Bay are impacted by anthropogenic activities, making studying ROM's behavior in these settings relevant. Tokyo Bay, located in the Kanto region of Japan, is one of the world's most heavily industrialized and urbanized areas, receiving substantial organic

matter inputs from various sources, including riverine discharge, wastewater treatment plant effluents, and atmospheric deposition [10].

Despite advancements in understanding DOC and FDOM dynamics, gaps still need to be identified, particularly in quantifying and characterizing persistent organic matter in urban coastal settings. Previous studies have primarily focused on the overall characterization of DOC and FDOM in Tokyo Bay, highlighting seasonal variations and the influence of different sources, such as riverine inputs and wastewater effluents. However, a more detailed understanding of ROM's composition, sources, and persistence in this highly urbanized coastal area still needs to be more detailed. Understanding the behavior and fate of ROM in Tokyo Bay is crucial for developing effective management strategies for urban coastal environments, especially considering the increasing anthropogenic pressures and climate change [11].

Operationally, the reactivity of DOC is determined by measuring its loss over a specific period [12]. However, there is no standard method for conducting these degradation experiments. Methodological variations further complicate the analysis, including differences in obtaining diluted seawater samples, such as the filters used in terms of composition and pore size, the ratio of the filtrate to inoculum, incubation temperature, light, and nutrient conditions, as well as the volume and duration of incubation. These factors reduce the reliability and comparability of data, necessitating careful consideration and interpretation of the results [13].

The final objective of this research is to analyze the characteristics and dynamics of RDOC in Tokyo Bay. To achieve this, several specific sub-objectives are established, including developing a method for estimating RDOC, clarifying the dynamics of RDOC in coastal areas, quantifying RDOC and LDOC removal during sewage treatment, calculating the total RDOC and LDOC influx through rivers, analyzing RDOC and LDOC concentrations in near-shore vs. whole-bay areas in different seasons, and assessing the proportion of RDOC in DOC for CO2 sequestration. This research holds significant value and innovation in understanding the dynamics of DOC in Tokyo Bay, particularly the refractory and labile fractions. It provides crucial insights into wastewater treatment plants' efficiency, human activities' impacts, and the broader environmental implications of DOC dynamics in urban coastal environments [14].

This research aims to provide insights into the dynamics of DOC in Tokyo Bay, particularly the refractory and labile fractions. Firstly, it compares the differences between RDOC and LDOC in sewage and effluents to evaluate the efficiency of wastewater treatment plants and identify areas for improvement. This comparative analysis helps evaluate the performance of these plants and guides enhancements in their processes to manage organic carbon loads better. By examining the RDOC and LDOC concentrations in the effluents from two different sewage treatment plants with three different treatments, this study uncovers variations in organic carbon removal efficiency and biological refractoriness among various treatment systems. These findings can assist policymakers in setting appropriate discharge standards and monitoring the environmental impact of effluents on the bay's ecosystem to improve environmental regulations and practices.

Secondly, the research calculates the total RDOC and LDOC entering Tokyo Bay through rivers to understand the trends and impacts of human activities and environmental factors on the bay's carbon budget. This understanding will aid future studies in identifying RDOC dynamics across various aquatic systems in Tokyo Bay, thereby contributing to a more thorough assessment of the region's carbon cycling and storage.

Thirdly, this study measures RDOC and LDOC concentrations in the often overlooked near-shore areas of Tokyo Bay. Understanding carbon cycling in these areas is crucial for assessing the overall carbon budget and ecosystem productivity of Tokyo Bay. The research also compared the effects of different filter pore sizes and incubation containers on RDOC ratio measurement, promoting the standardization of DOC reactivity research.

An additional aspect of this research is the extensive sampling strategy that spans several months, including periods following summer typhoons. This allows for assessing seasonal variations and the impact of extreme weather events on DOC dynamics in Tokyo Bay. By capturing data across different seasons and after significant weather events, the study can infer the seasonal changes in the DOC pool and how events like typhoons affect the transport and transformation of DOC. This aspect of the study aims to enhance understanding of the temporal variability in carbon dynamics and the influence of climatic factors on DOC in coastal ecosystems.

1.2. Literature review

Operationally, the reactivity of dissolved organic carbon (DOC) is assessed by monitoring its reduction over a specified timeframe (Giorgio & Davis, 2003). The biologically labile fraction is identified as DOC degraded within hours to days, the semi-labile fraction within weeks to months, and the semi-refractory fraction over years to decades. Seawater samples undergo incubation in controlled laboratory settings for periods ranging from days to years to analyze the breakdown rates of organic matter and determine the refractory DOC remaining in the environment (Lønborg & Álvarez-Salgado, 2012).

However, a standardized method for these degradation experiments does not exist. The incubation time and conditions influence the DOC concentration and degradation rate, complicating data comparison and collection (Robinson et al., 2018). For example, N. Ogura (1975) conducted degradation experiments using 1.2 μm GF/C filters and incubated samples in 300 ml glass bottles for 30 to 40 days. Later, Peter et al. (2000) used baked 142 mm diameter GF/D filters (pore size 2.7 μm) and GF/F glass fiber filters (pore size 0.7 μm) to sequentially filter the samples and incubated water in 1 L polycarbonate bottles for 28 days. In 2010, He et al. performed short-term (1-3 days) in situ incubations, filtering water samples through acid-washed cartridge filters (~1 μm pore size) and collecting the samples into a 20 L pre-cleaned carboy, with final filtering through 0.7 μm GF/F filters before DOC concentration determination. Kubo et al. (2015) filtered samples with GF/F filters (0.7 μm) and incubated the filtrates in 600 mL amber glass bottles for 150 days. In 2020, Watanabe et al. conducted field-bag degradation

experiments by filtering samples through pre-combusted GF/F glass fiber filters and incubating them in 100 mL glass vials for 150 days. Post-incubation, samples were filtered through 0.2 μm polytetrafluoroethylene filters and stored at -20°C until analysis.

Variations in methodology further complicate the analysis, including differences in the filters used (composition and pore size), filtrate-to-inoculum ratio, incubation temperature, light, and nutrient conditions, and the volume and duration of incubation. These variations reduce data reliability and comparability, necessitating careful consideration and interpretation of results.

There is a pressing need for cross-comparison of methods and recommendations for standardization in DOC degradation research (Baltar et al., 2021). Establishing a standard method would facilitate systematic laboratory-scale bioassay experiments to assess the impact of various environmental conditions, such as light, temperature, and nutrients, on DOC degradation (Robinson et al., 2018).

The selection of filter pore size significantly affects DOC degradation results, influencing both DOC compounds and bacteria in the filtrates. Denis et al. (2017) examined the effect of different filter selections ranging from 0.2 to 0.7 μm on the concentration and composition of dissolved organic matter (DOM), finding no significant difference for bulk scale descriptors and at the molecular scale. Conversely, Dean et al. (2018) investigated the impact of filter size on bacterial community composition and DOM degradation dynamics using three strategies: 0.2 μm, 0.7 μm, and 106 μm (unfiltered). Their findings indicated that bacterial community composition and DOM degradation dynamics were influenced by filtration strategy, mainly affecting bio-lability assays through bacterial abundance and the presence of their associated predators.

Including different size classes of DOM can also affect microbial degradation. Amon and Benner (1996) observed that high-molecular-weight DOC was more utilized than low-molecular-weight DOC across various environments. Filters smaller than 0.7 μm could potentially remove most bacteria, overestimating the refractory dissolved organic carbon ratio since bacteria in water typically range from 0.5 to 2 μm in diameter (Fenchel et al., 2012).

Previous research on dissolved organic carbon (DOC) and refractory dissolved organic carbon (RDOC) in Tokyo Bay has primarily focused on understanding their spatial and temporal variations, sources, and behavior in this highly urbanized coastal water. Kubo et al. (2023) conducted a comprehensive study from June 2013 to April 2014, which included monthly water sample collections from various stations, including the Arakawa River and sewage treatment plant (STP) effluents. Their analysis revealed consistently higher RDOC concentrations than labile DOC (LDOC) across all seasons and stations, with RDOC primarily derived from STP effluents. To estimate fluorescent dissolved organic matter (FDOM), they utilized an Excitation Emission Matrix (EEM) combined with Parallel Factor Analysis (PARAFAC), identifying six fluorescent components characterized as humic-like and tryptophan-like substances, most of which were biologically recalcitrant. Degradation experiments indicated that RDOC concentrations remained stable while LDOC was rapidly decomposed by bacterial activity. Linear relationships between FDOM components and salinity suggested that the majority of FDOM in Tokyo Bay originated from STP effluents rather than phytoplankton. Principal Component Analysis (PCA) demonstrated that recalcitrant substances with high aromaticity were mainly associated

with STP effluents, whereas both STP effluents and in-situ bacterial production influenced bioavailable substances. Despite significant progress, several areas require further investigation. These include a deeper analysis of LDOC sources, the impact of photodegradation on DOC and RDOC, the effects of seasonal and episodic events such as heavy rainfall on DOC dynamics, and the effectiveness of advanced STP treatment processes in reducing RDOC and LDOC loads. Future research should address these gaps to enhance the understanding of DOC and RDOC dynamics in urbanized coastal ecosystems like Tokyo Bay (Kubo et al., 2023).

1.3. Research Objectives

The primary objective of this research is to understand the spatiotemporal distribution and behavior of RDOC in Tokyo Bay. To achieve this, the following specific sub-objectives are established:

1. Develop a Method for Estimating RDOC
2. Clarify the Dynamics of RDOC in Coastal Areas
3. Quantify RDOC and LDOC Removal During Sewage Treatment
4. Calculate Total RDOC and LDOC Influx Through Rivers
5. Analyze RDOC and LDOC Concentrations in Near-Shore vs. Whole-Bay Areas
6. Assess the Proportion of RDOC in DOC for CO2 Sequestration
7. Investigate Organic Substances in DOC

2. Methodology

A comprehensive approach will be adopted to achieve the outlined sub-objectives. First, a method for estimating RDOC in marine environments will be developed by analyzing seawater samples' fluorescence and UV-visible absorption spectra to assess FDOM and Colored Dissolved Organic Matter (CDOM), providing quicker and more efficient RDOC evaluations without lengthy decomposition tests. The spatial and temporal dynamics of RDOC in Tokyo Bay will be investigated by analyzing distribution patterns and persistence across different regions and seasons, revealing the processes involved in RDOC formation and sequestration. The removal efficiency of RDOC and LDOC during sewage treatment processes will be determined to evaluate the effectiveness of current wastewater treatment practices in reducing DOC levels before discharge into coastal waters. Additionally, the total amount of RDOC and LDOC flowing into Tokyo Bay through rivers will be calculated and compared with historical data, assessing changes in DOC influx over time and the effectiveness of measures to reduce DOC input from

riverine sources. Comparative analysis of RDOC and LDOC concentrations in near-shore areas versus the middle of the bay will provide insights into DOC distribution patterns and the impact of different sources and environmental processes. The proportion of RDOC in DOC will be quantified to assess the ocean's capacity to sequester atmospheric CO2, understanding the transformation of LDOC into dissolved inorganic carbon (DIC) and its potential re-emission as CO2. Lastly, the study will differentiate various organic substances in DOC, such as humic and fulvic acids from vegetation and proteins and amino acids from sewage, analyzing their fluorescence and absorption characteristics to better understand their contributions to the overall DOC pool in Tokyo Bay.

2.1. Study area

This study focuses on the concentration and reactivity of DOC in Tokyo Bay, Japan. Tokyo Bay is a partially enclosed water body that spans approximately 922 square kilometers and has an average depth of 19 meters [15]. Located in central Japan, the bay is surrounded by densely populated urban areas with a population of about 29 million. The estimated water residence time in Tokyo Bay is around 50 days [16]. Due to its heavy urbanization, Tokyo Bay faces environmental challenges like other coastal regions [16].

Water samples and effluents were collected from the lower river stations downstream of the Arakawa and Edo Rivers just before they reached Tokyo Bay. The Arakawa River, originating from the Chichibu Mountains, flows through the Kanto region, including Tokyo, before emptying into Tokyo Bay after a journey of approximately 173 kilometers [17]. The Kasai Water Reclamation Center near its mouth is crucial for treating wastewater and maintaining water quality before discharge into the bay [17].

The Edo River, another significant river in the Kanto region, stretches about 59 kilometers from its source in the Tone River system. It flows through Chiba and Tokyo before reaching Tokyo Bay [18]. The Edogawa Second Final Treatment Plant, located along this river, manages and treats wastewater from the surrounding urban areas, ensuring that effluents released into the bay comply with environmental standards [18].

For this study, water samples were collected from the lower reaches of the Arakawa and Edo Rivers and various points within Tokyo Bay. Nineteen samples were collected using a boat, allowing for an analysis of the distribution and sources of DOC within Tokyo Bay, covering both terrestrial and marine environments. The sampling locations and sites are illustrated in Figure 2.1 and detailed in Table 2.1.

DOC concentration and reactivity were analyzed using standard laboratory procedures. To remove particulate matter, water samples were filtered through pre-combusted GF/F filters (0.7 μm pore size). DOC concentrations were measured using high-temperature catalytic oxidation with a total organic carbon analyzer [19]. Reactivity experiments involved incubating water samples under controlled laboratory conditions to determine the rate of DOC degradation [20].

Data analysis included calculating DOC concentrations and reactivity rates for all samples. Statistical analysis was performed to identify spatial and temporal patterns in DOC distribution and determine various sources' influence on DOC levels in Tokyo Bay. The results were used to assess the effectiveness of urban water management practices in controlling DOC inputs into the bay [16].

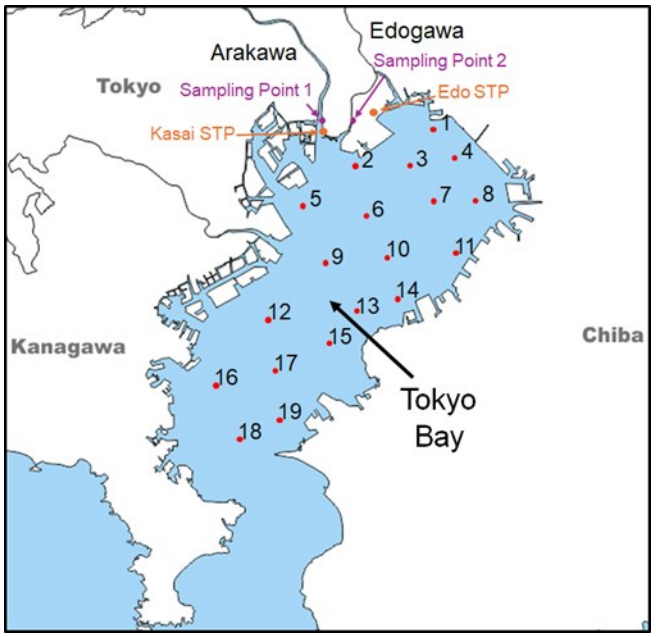

Figure 2.1 Study Area

Table 2.1 The latitude and longitude of each site

Sampling site	latitude	longitude
Kasai STP	35.64882	139.5885
Edo STP	35.67959	139.9098
Sampling Point 1 (lower Arakawa)	35.65528	139.8501
Sampling Point 2 (lower Edogawa)	35.66410	139.8873
Kasai STP	35.64882	139.5885
Edo STP	35.67959	139.9098
Sampling Point 1	35.65528	139.8501
Sampling Point 2	35.66410	139.8873
1	35.65529	139.8501
2	35.66411	139.8874
3	35.64773	139.9938
4	35.61206	139.8956
5	35.60032	139.9655
6	35.61910	140.0290
7	35.56605	139.8379
8	35.55477	139.9037
9	35.56464	139.9845
10	35.56651	140.0538
11	35.51530	139.8587
12	35.51295	139.9291
13	35.51530	140.0192
14	35.45795	139.7749
15	35.45936	139.8766

2.2. Field survey

Water samples were gathered from different marine environments to analyze the RDOC ratio, and experiments were carried out to study the degradation of DOC. Samples were taken from river water and near-shore locations at the surface level, as illustrated in Figure 2.2. The sampling schedule can be found in detail in Table 2.2. River water samples, taken fourteen times between February 2023 and May 2024, were collected from the lower stretches of the Arakawa River and the Edo River. These sampling points were both upstream and downstream from the discharge locations of sewage treatment plant effluents. The samples were obtained using a plastic bucket and rinsed with sample water three times before use, as shown in Figure 2.2a. Additionally, sewage treatment plant (STP) samples, which included both sewage and effluent, were collected four times by staff from the Kasai and Edo STPs between April 2023 and February 2024. In September 2023, 19 samples were collected from the surface of Tokyo Bay using a research vessel representing various locations across the bay. Here, we use AAQ, a water quality detector that allows faster and more efficient water quality profiling. A sampler and AAQ were utilized to collect the surface layer water for these samples, as shown in Figure 2.2b.

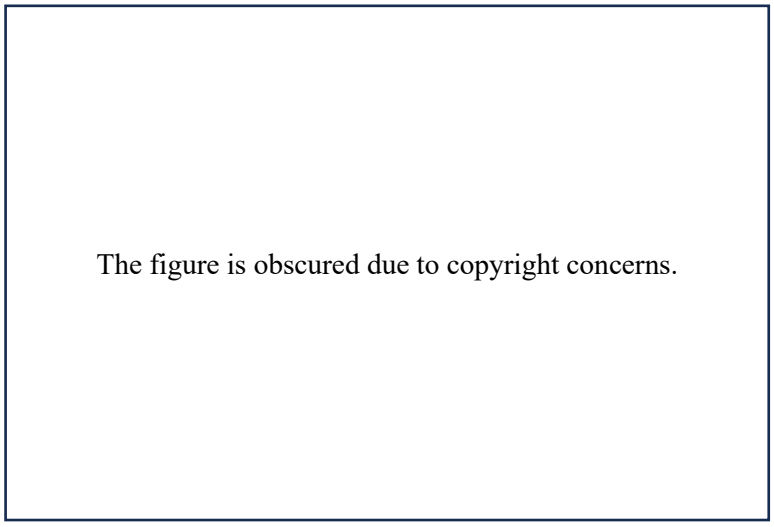

Figure 2.2 Sampling method. Bucket sampling (a) Sampler and AAQ (b)

During sampling, the water quality meter (JFE Advantech Corporation) with plate number AAQ-177 was used for direct measurement. The water sampler was attached to a rope to measure water quality parameters while collecting samples. All samples, whether collected using the sampler or bucket, were transferred into 1-liter brown bottles (refer to Fig. 2.2). These bottles were cleaned beforehand with an ultrasonic cleaner and HCl, then heated to 550°C for 10 hours and lastly rinsed with Milli-Q water. Afterward, the bottles were stored in the dark until processed in the laboratory.

Figure 2.3 Brown glass bottles

Nineteen samples of Tokyo Bay were collected during the boat survey (Fig. 2.4) on 20th September 2023.

Figure 2.4 Boat Survey on Tokyo Bay

Table 2.2 Sampling Schedule

Source	Sampling Sites	Sampling Datetime
Kasai STP	Sewage	Feb. 22nd. 2023 May. 25th. 2023 Aug. 22nd. 2023 Jan. 31st. 2024
Kasai STP	Effluent	Feb. 22nd. 2023 May. 25th. 2023 Aug. 22nd. 2023 Jan. 31st. 2024
Edo STP	Sewage	Feb. 22nd. 2023 Aug. 22nd. 2023 Jan. 31st. 2024
Edo STP	Effluent East	Feb. 22nd. 2023 Aug. 22nd. 2023 Jan. 31st. 2024
Edo STP	Effluent 1-8	Feb. 22nd. 2023 Aug. 22nd. 2023 Jan. 31st. 2024
River water	Lower Arakawa River	Feb. 22nd. 2023 May. 25th. 2023 Jun. 18th. 2023 Jul. 28th. 2023 Aug. 22nd. 2023 Sept. 9th. 2023 Oct. 25th. 2023 Dec. 5th. 2023 (Nov Samples) Dec. 25th. 2023 Jan. 31st. 2024 Feb. 29th. 2024

		Mar. 23rd. 2024 Apr. 25th. 2024 May. 30th. 2024
River water	Lower Edogawa River	Feb. 22nd. 2023 May. 25th. 2023 Jun. 18th. 2023 Jul. 28th. 2023 Aug. 22nd. 2023 Sept. 9th. 2023 Oct. 25th. 2023 Dec. 5th. 2023 (Nov Samples) Dec. 25th. 2023 Jan. 31st. 2024 Feb. 29th. 2024 Mar. 23rd. 2024 Apr. 25th. 2024 May. 30th. 2024
Tokyo bay	Tokyo bay	Sept. 20th. 2023 Mar. 5th. 2024

The sampling schedule for this study is outlined in Table 2.2. Samples from the Kasai STP (Sewage Treatment Plant) and Edo STP, which include both sewage and effluent, were collected in February 2023, May 2023, August 2023, and January 2024. River water samples from the lower Arakawa and lower Edo rivers were collected monthly from April 2023 to May 2024, ensuring a consistent and comprehensive data collection. Additionally, samples from Tokyo Bay were collected on September 20, 2023. For degradation experiments, samples were collected twice from the lower Arakawa River station and near-shore areas near the Arakawa River estuary. These sample collection procedures adhered to the methodologies previously described.

On each sampling occasion, water samples were carefully transferred to 1-liter polycarbonate bottles and immediately filtered through GF/F filters pre-combusted at 500°C for 5 hours to ensure cleanliness and prevent contamination. After filtration, DOC and FDOM samples were transferred to 1-liter brown glass bottles, pre-soaked in hydrochloric acid, and baked at 550°C for 10 hours. This stringent preparation was essential to avoid any potential interference from residual organic material.

Some FDOM samples were transferred to 10 ml plastic test tubes treated with hydrochloric acid and then frozen until analysis to preserve their integrity. Due to instability in the experimental instruments in later experiments, some DOC samples were transferred to 60 ml glass bottles and plastic sampling bottles treated with hydrochloric acid. These samples were then frozen in laboratory cold storage until analysis to ensure their preservation. The procedures for handling and preserving these samples are depicted in Figure 2.5, illustrating the meticulous care taken at each step to maintain the samples' quality and reliability for subsequent analysis.

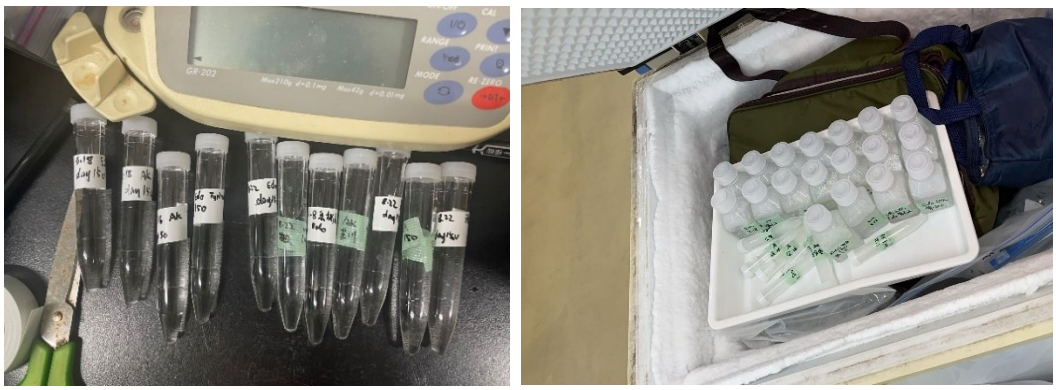

Figure 2.5 Preserved sample

Table 2.3 Sampling Schedule for evaluating the accuracy

Sampling Sites	Sampling Datetime
Lower Arakawa River	Feb. 22nd. 2023, Apr. 24th. 2023
Near-shore Area	Feb. 22nd. 2023, Apr. 24th. 2023

Table 2.3 displays the sampling schedule for a degradation experiment. The experiment evaluated the impact of various filter pore sizes and container volumes under identical incubation conditions.

2.3. Degradation experiment

Experiments were conducted to investigate the decomposition of dissolved organic carbon in controlled conditions, which is essential for determining the reactive dissolved organic carbon ratio in specific water bodies.

2.3.1. Incubation of samples for microbial degradation

Several preliminary trials were conducted before the formal experiments commenced to compare different filters and incubation containers. Within 24 hours of collection, the water samples were filtered using 0.45 μm GD/X filters in the lab and then transferred into 50 mL glass vials. These vials underwent a rigorous preparation process: they were prewashed with an ultrasonic cleaner and hydrochloric acid (HCl), pre-combusted at 550°C for 10 hours to eliminate any organic contaminants, and rinsed thoroughly with Milli-Q water. The vials were then sealed with rubber and aluminum caps to maintain sample integrity.

Frequent replacement of filters was necessary to mitigate cell lysis and filter clogging caused by the high particulate organic matter (POM) load, a common issue in water samples with significant organic content [21]. GD/X filters were chosen for their efficacy, though it is acknowledged that they allow many free-living bacteria to pass into DOC samples [22][23]. The filtered samples were stored at room temperature (20°C) in complete darkness until analysis. All vials were covered with aluminum foil to ensure a light-free environment, as illustrated in Figure 2.6.

Each vial contained 20 mL subsamples for incubation, with a 30 mL headspace containing approximately 270 μmol of oxygen. This setup was designed to ensure sufficient oxygen availability for bacterial heterotrophic decomposition. Based on established literature, the study assumed that 1 mol of oxygen would be consumed for each mol of organic carbon mineralized into CO_2 [23][24]. This study's highest initial DOC concentration was 2988 μmol L^{-1}, ensuring that the headspace oxygen was adequate for the expected mineralization process.

The degradation experiments included seven distinct incubation periods: 0, 2, 5, 10, 20, 30, and 50 days for each field sampling event.

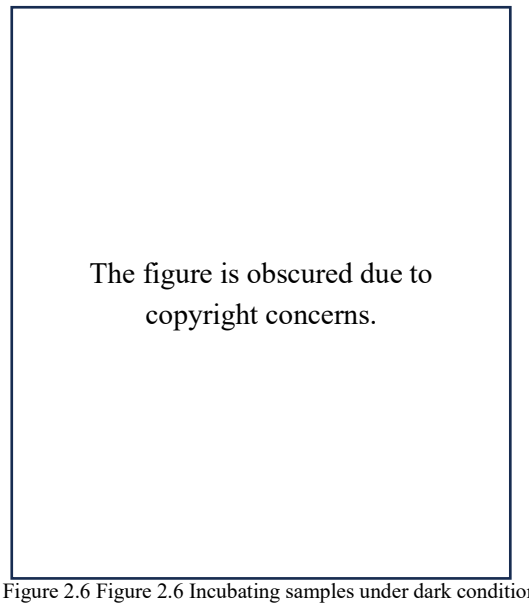

Figure 2.6 Figure 2.6 Incubating samples under dark condition

This study defined RDOC as the DOC concentration remaining after 50 days of incubation, a period chosen based on previous studies indicating significant microbial degradation within this timeframe [25]. LDOC was determined by subtracting RDOC from the initial DOC concentration. These degradation experiments were specifically designed to focus on microbial degradation processes, consistent with methodologies used in similar studies to distinguish between different fractions of DOC [26][27].

After comparing 0.45 µm GD/X and 0.7 µm GF/F filters, as well as 50 mL and 1 L incubation containers, the 0.7 µm GF/F filter and 1 L brown glass bottles were chosen as the final experimental equipment, as shown in Figure 2.7.

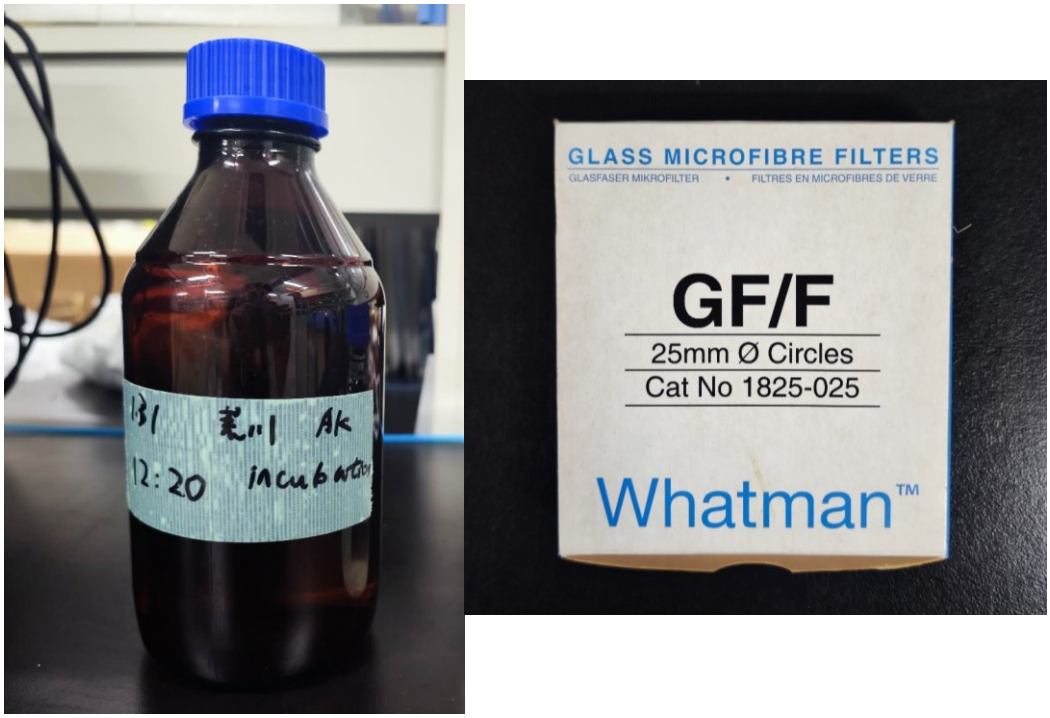

Figure 2.7 Water filtering bottle and microfibre filters

The preliminary experiments used the 50-day degradation experiment results to determine the final RDOC. However, the final degradation experiment was extended to 150 days to ensure rigor. The degradation experiments included nine time points: 0, 2, 5, 10, 20, 30, 50, 100, and 150 days for each field sampling event. The highest initial DOC concentration in this study was 2988 µmolL-1. If we assume that 1 mol of oxygen is consumed when 1 mol of organic carbon is mineralized into CO2, the oxygen in headspace should have provided a sufficient oxygen supply for heterotrophic decomposition by bacteria (Kubo et al., 2015; Watanabe et al., 2020). The degradation experiments were conducted based on seven incubations (0, 2, 5, 10, 20, 30, and 50 days) per field sampling event. To ensure sufficient sample volume for the 150-day duration, 900 mL was collected during each sampling event. Calculations indicated that the 150 mL of air left in the bottle headspace was sufficient for the microbial degradation of DOC, as approximately 80 mL of the sample was removed during each subsequent experiment. Of the 80 mL, 20 mL was used to rinse the experimental tubes, and the remaining 60 mL was divided into

three aliquots for analysis. Each removal introduced new air and created additional headspace, facilitating ongoing microbial activity.

The oxygen requirement was calculated for a wastewater treatment plant's DOC concentration of 3854 μmol L^{-1} in a 1 L bottle to determine the necessary headspace for a different DOC concentration.

First, the total DOC in the sample was calculated:

$$\text{DOC concentration} = 3854\ \mu\text{mol/L}$$

Given a 1 L bottle, the total DOC is:

$$\text{Total DOC} = 3854\ \mu\text{mol}$$

Next, the amount of oxygen required for mineralization was determined. Based on the assumption that 1 mol of oxygen is consumed for each mol of DOC:

$$\text{Oxygen required} = 3854\ \mu\text{mol}$$

Finally, the headspace needed to contain the required oxygen was calculated. Let V denote the volume of headspace in liters. Assuming the molar volume of gas at laboratory conditions is approximately 24 L/mol, the volume of O_2 required is:

$$\text{Te volume of O2 required} = \frac{3854\ \mu\text{mol}}{1000000} \times 24\ \text{L/mol} \approx 0.0925\text{L}$$

Thus, to ensure sufficient oxygen for the mineralization of 3854 μmol L^{-1} of DOC in a 1 L bottle, a headspace of approximately 0.0925 liters (or 92.5 mL) should be reserved.

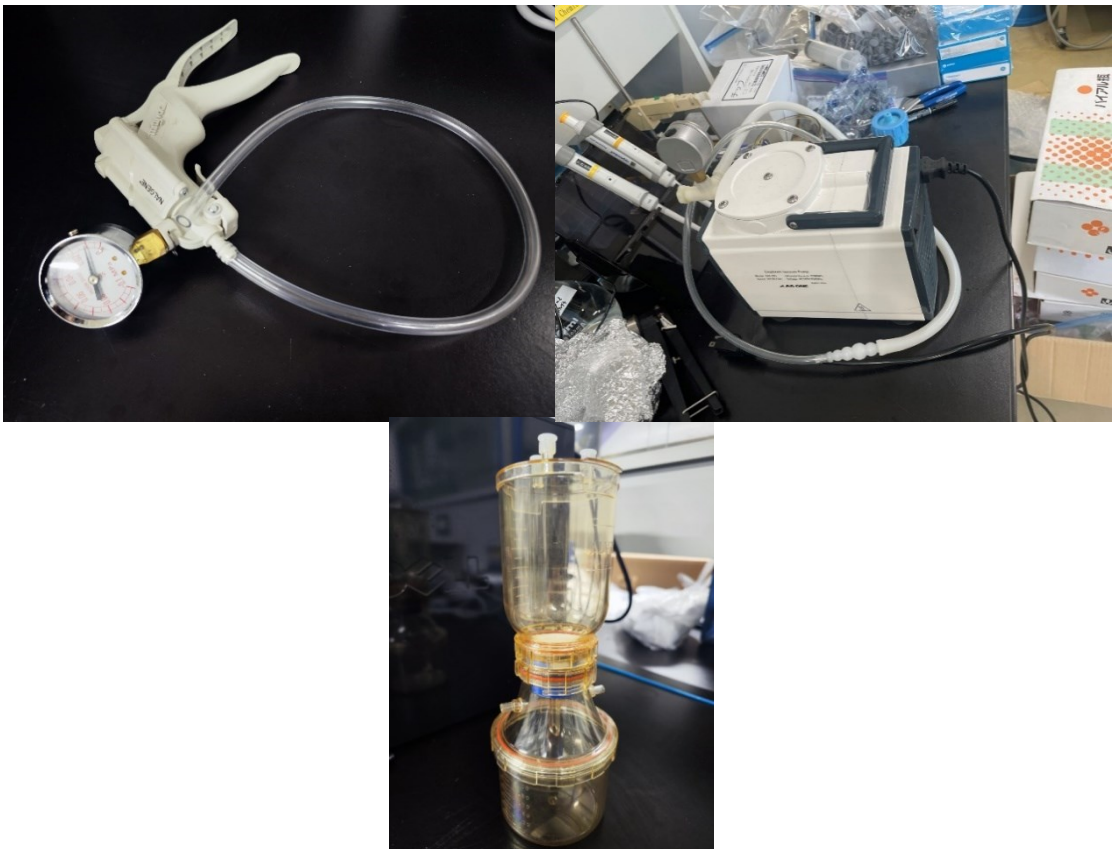

Figure 2.8 Manual vacuum pump, Electric vacuum pump and Filter

The research utilized 1-liter amber glass bottles and 0.7 μm GF/F filters for experiments. Initially, due to a limited number of samples before August 2023, a manual vacuum pump, as illustrated in Figure 2.8a, was employed for filtration. However, upon entering a ship-based sampling expedition in September, manual and electric vacuum pumps, as shown in Figures 2.8a and 2.8b, were used to handle the increased sample volume. Additionally, Figure 2.8c depicts the type of filter used during each filtration process. This combination of manual and electric vacuum pumps allowed efficient and effective sample collection and processing during the research period.

2.3.2. Measuring samples with TOC-VCPH/CPN

After the incubation period, DOC samples were analyzed in triplicate using a Total Organic Carbon (TOC) analyzer (TOC-VCPH/CPN, Shimadzu, Japan) (Fig. 2.9).

Figure 2.9 Total Organic Carbon Analyzer (Left is automatic sampler)

A potassium phthalate solution measured the DOC. Considering the influence of the Total Organic Carbon (TOC) analyzer blank, pure water, and any carbon derived from vials, the DOC measurement's precision was approximately 4.8%. This precision was tested using a designed experiment and calculated using the following formula:

$$precision = \frac{Value_{max} - Value_{min}}{2 * Average\ value}$$

The unit transformation applies from μg/L to micromoles per liter (μmol/L) to get a straight view of the results. Those two units are marked as Old and New, respectively. The transformation follows this formula:

$$New = \frac{Old * 1000}{12.01}$$

The TOC analyzer operates based on the non-dispersive infrared (NDIR) method, a widely used technique for analyzing organic carbon in various samples. The analyzer consists of several key components: a sample introduction system, an oxidation reactor, a CO_2 gas detection system, and a data acquisition and analysis system.

The analysis process begins with the sample introduction system, which ensures the accurate and precise delivery of the sample into the analyzer. Once introduced, the sample passes through the oxidation reactor, where organic carbon compounds are oxidized to form carbon dioxide. This oxidation typically occurs via high-temperature combustion or chemical oxidation. The resulting CO_2 gas is then directed to the CO_2 gas detection system, where its concentration is measured using the NDIR technique. This method involves the absorption of infrared light by CO_2 molecules, with the decrease in light intensity being proportional to the CO_2 concentration. The TOC analyzer's data acquisition and analysis system collects the CO_2 concentration data. It calculates the corresponding TOC concentration in the original sample by applying a calibration curve obtained from TOC standards.

The main procedure for processing DOC measurements includes:

A. Calibration and Standardization: Prepare a series of standard solutions with known concentrations of organic carbon (0, 5, 10, 20 mg/L before February 22, 2023, and 0, 1, 2, 5, 10, 20 mg/L after February 22, 2023). These standards calibrate the TOC analyzer and establish a calibration curve for accurate DOC quantification. Before April 1, 2023, standard solutions were made daily. After April 1, 2023, each different standard solution was prepared in 100ml quantities and stored in a refrigerator to minimize errors from manual preparation each time.(Fig. 2.10).

B. Preparation of Samples: Transfer subsamples into specially washed 20 mL vials using an ultrasonic cleaner and HCL. Then, the vials and standard solutions are placed into the sampler connected to the TOC analyzer. Set up the TOC Analyzer by creating calibration and method files, inputting the sample measurement sequence, starting the machine, and beginning the analysis.

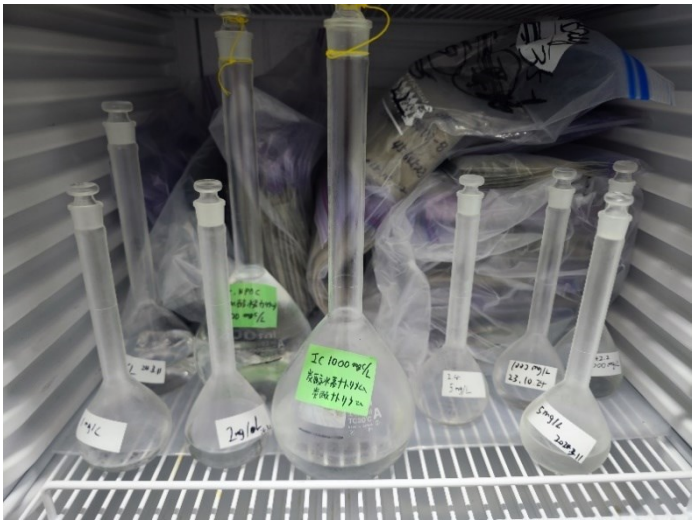

Figure 2.10 Standard solution

As the TOC analyzer is old, it is necessary to check the machine's performance and identify factors that might influence the precision of the results. Based on all the experiments conducted using the TOC analyzer, two factors were found to influence the precision of the results:

1. When high-concentration samples (e.g., 20 μmol L-1) are measured, subsequent samples might be contaminated by residual liquid in the machine.
2. Residual liquid in the tube connecting the sampler and the TOC analyzer can affect adjacent samples.

To clarify these two factors, an exploratory experiment was designed.

Under normal circumstances, the interior of the experimental equipment is washed once with Milli-Q water from a large bottle between every two samples. In the control experiment, a small vial filled with Milli-Q water was placed between different samples, meaning it could clean not only the interior of the machine but also the tube connecting the sampler and the machine.

The following conclusions were drawn based on the results: The effect of high-concentration samples can be eliminated by washing both the tube and the machine's interior once. Most DOC measurements for Milli-Q (n) were higher than for Milli-Q (0), indicating that residual liquid in the tube indeed has an effect. Therefore, it is advisable to wash not only the interior of the machine but also the tube before each sample measurement. In subsequent measurements, the machine's interior was washed twice with Milli-Q water, and the tube was washed once before and after each measurement. Additionally, between measurements of different samples, the interior of the machine and the tube were cleaned with Milli-Q water from the small vial. Although efforts were made to minimize the influence between standard solutions and different samples during the experiment, some instability in the machine remains. Hence, each sample was evenly divided into two parts after thorough mixing: one part for immediate analysis and the other stored in the refrigerator for the next round of experiments, allowing for correction of the results.

For example, the sample from day 0 was divided into two parts. On May 10th, the DOC was measured, yielding a result of 163. The backup portion was thawed and measured along with the second

day's sample on May 12th, yielding results of 157 and 149, respectively. With these two different results for the same sample, a correction algorithm can be applied:

$$D_2' = \frac{D_0^{(1)}}{D_0^{(2)}} \times D_2$$

$D_0^{(1)}$ is the DOC value of the day zero sample measured on May 10th.

$D_0^{(2)}$ is the DOC value of the day zero sample measured on May 12th.

D_2 is the DOC value of the day two sample measured on May 12th.

D_2' is the corrected actual DOC value of the day two sample.

Thus, the DOC measurements can be corrected using this equation to account for any discrepancies.

2.4. Carbonic analysis

The concentration of dissolved inorganic carbon (DIC) and total alkalinity (TA) were measured using the total alkalinity titration machine (ATT-05; Kimoto Electric, Osaka, Japan) (Fig. 2.11).

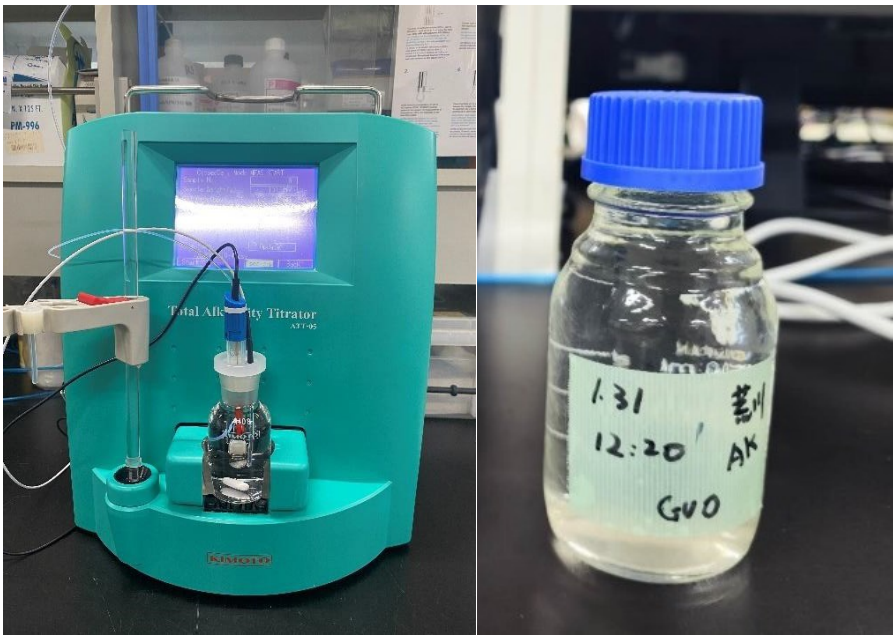

Figure 2.11 ATT-05(left) and ATT sample(right)

The titration method relies on the principle of neutralization titration and can be performed using either the open-cell or closed-cell methods. The open-cell method uses the ATT-05 to inject acid until the pH reaches a degassing point quickly, then proceeds with titration to measure total alkalinity (TA), excluding the influence of carbonates. In contrast, the closed-cell method involves titrating the seawater sample with carbonates present, allowing for the simultaneous measurement of total alkalinity and total dissolved inorganic carbon (DIC).

For this study, the closed-cell method was chosen to measure both TA and DIC to ensure accuracy. Before measuring the samples, ordinary seawater was tested until the ATT-05 readings stabilized. Additionally, MCR solutions were measured both before and after the sample measurements. MCR, a standardized solution with known concentrations of specific chemical compounds or elements, is used as a calibration solution in ATT-05 measurements. This standardized solution helps establish a reference point for the instrument's measurement scale. By analyzing the MCR solution, the ATT-05 can determine its response and make necessary adjustments to ensure precise and reliable measurements.

Sample preparation is a crucial step to ensure the accuracy and reliability of the measurements. During sampling, 250 mL white glass bottles were rinsed with the sample to precondition them. Then, the liquid sample was filled into the glass bottle until it was complete without overflowing. Mercuric chloride was then added to preserve the sample. On the workbench, gloves and masks were worn to ensure safety and prevent contamination. A pipette added 200 μL of mercuric chloride to the filled sample bottle. The bottle was then capped and shaken to dissolve the mercuric chloride thoroughly.

Adding mercuric chloride is essential to prevent biological activity, such as the growth of microorganisms, which could alter the sample's chemical composition before analysis. Biological processes can consume or produce carbon dioxide, leading to inaccurate dissolved inorganic carbon (DIC) measurements and total alkalinity (TA). Mercuric chloride helps maintain the sample's integrity by inhibiting these biological processes.

Several studies support this practice, which is a standard method in oceanographic research. For instance, Dickson et al. (2007) recommend using mercuric chloride to preserve seawater samples intended for carbonate system measurements, noting its effectiveness in preventing biological activity and ensuring accurate results [28].

2.5. Analysis of fluorescence excitation-emission matrices (EEMs)

In my research, conducted in collaboration with the Precision Instrument Laboratory at Yokohama National University, two advanced instruments provided by Yokohama National University were used to measure the fluorescence characteristics of compounds in each sample on Day 0 and Day 150. The specific instruments used were the UV-Vis spectrophotometer (V-560, JASCO, Japan) and the fluorescence spectrophotometer (FP-8500, JASCO, Japan).

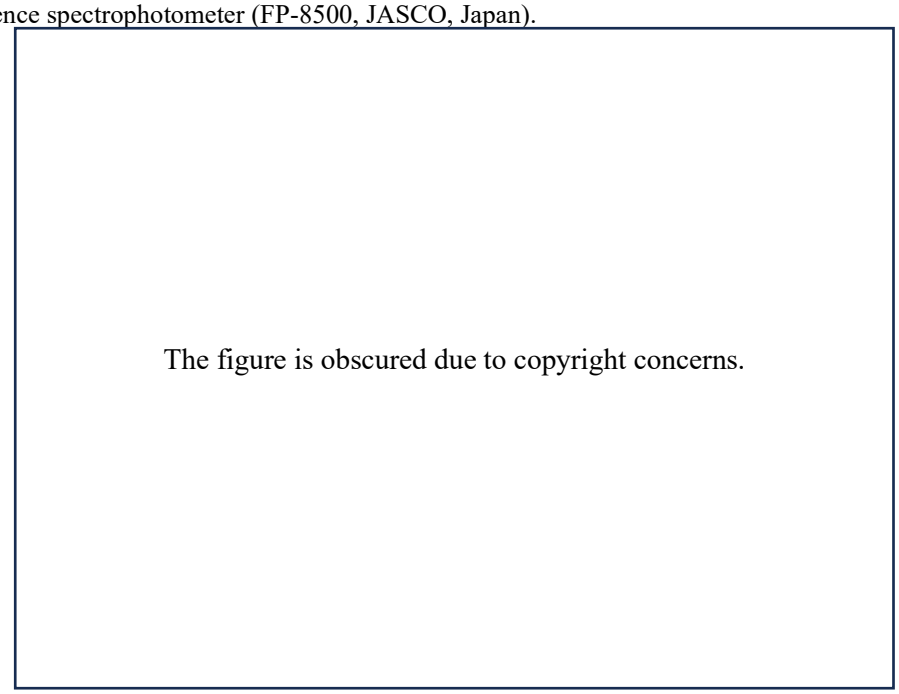

Figure 2.12 Spectrophotometer(V-560)

The UV-Vis spectrophotometer (Model: V-560) by JASCO is employed to measure the optical properties of compounds and perform quantitative analysis as per official methods. It measures the absorbance of solutions and thin films in the ultraviolet to visible light range (190-900 nm). This double-beam system provides higher stability than single-beam systems, making it suitable for research. The instrument is utilized to evaluate the optical properties of substances and plays a significant role in investigating the thickness of thin films and the arrangement of colloidal crystals.

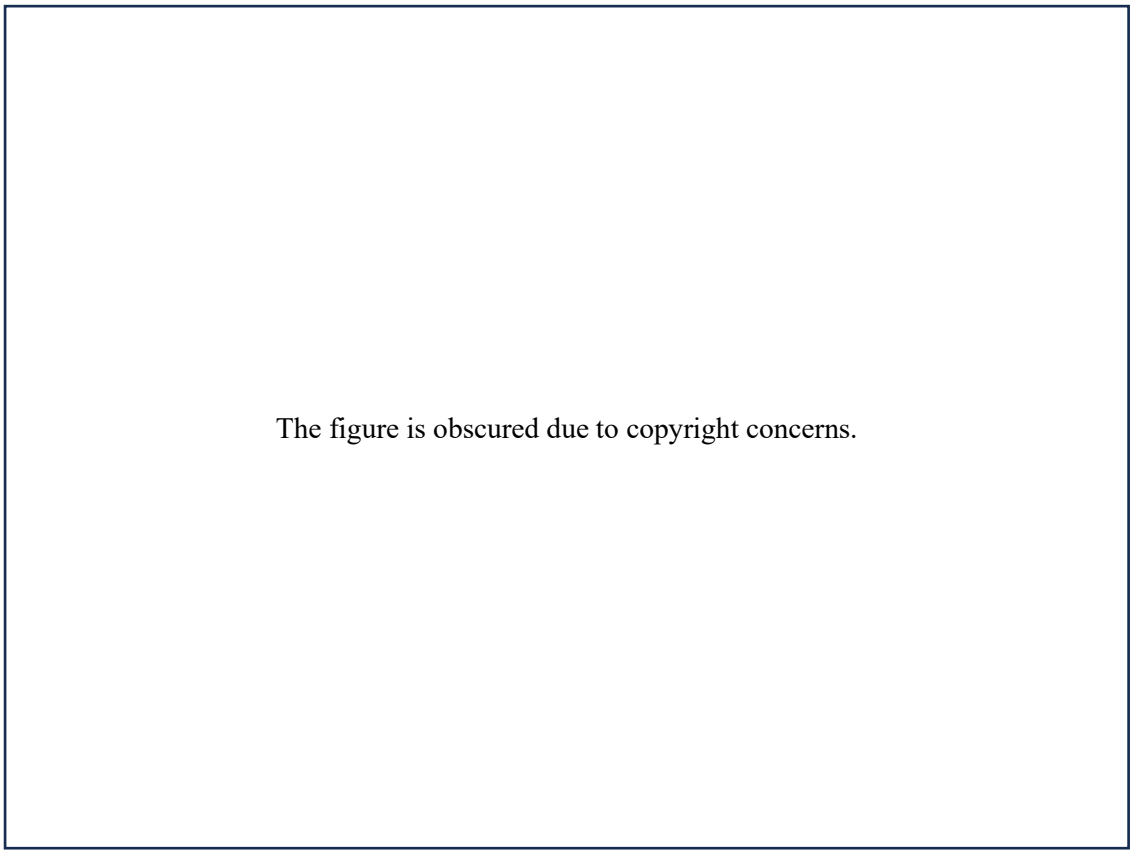

Figure 2.13 Using spectrophotometer

JASCO's fluorescence spectrophotometer (Model: FP-8500) is used for luminescence analysis (ultraviolet to visible light) in solutions and bulk materials. Luminescence refers to the phenomenon where energy excited by electromagnetic waves or heat is emitted as light of specific wavelengths. This instrument measures photoluminescence resulting from the absorption of ultraviolet and visible light. One key feature of fluorescence spectroscopy is its higher sensitivity than absorption spectra obtained through differential measurements. Additionally, since only specific samples exhibit fluorescence, this characteristic can be leveraged for high selectivity in analyses.

The UV-Vis spectrophotometer (V-560, JASCO, Japan) and the fluorescence spectrophotometer (FP-8500, JASCO, Japan) played crucial roles in measuring the optical and fluorescence properties of the samples. The V-560 measured absorbance in the UV-visible range (190–900 nm) with high stability and accuracy, while the FP-8500 provided high sensitivity for fluorescence measurements, allowing for precise analysis of the fluorescence properties and quantum yields of the samples. EEMs covered excitation wavelengths from 250–550 nm at 5 nm intervals and emission wavelengths from 290–600 nm at 2 nm intervals. EEM spectra were normalized to Raman units by correcting the area under the Raman scattering peak at 350 nm of excitation, and the Raman normalized MilliQ water EEM spectrum was subtracted from the EEM spectra of samples to remove water Raman scattering. The fluorescence features in EEMs were decomposed into individual components using parallel factor analysis (PARAFAC).

For sample preparation, samples were filtered through 0.7 μm GF/F filters to remove particulate matter and stored in the dark at four °C until analysis. This step prevents any photochemical changes in the samples that could affect the fluorescence measurements. EEMs were collected for each sample, covering excitation wavelengths from 250 to 550 nm and emission wavelengths from 290 to 600 nm. This range was selected to capture the significant fluorescence peaks associated with various types of dissolved organic matter.

Data analysis employed PARAFAC to decompose EEM data into individual fluorescent components, each representing different types of FDOM. PARAFAC is a statistical tool that helps identify and quantify distinct fluorescent components within complex mixtures of dissolved organic matter. The EEM data were processed and analyzed using the DOMFluor toolbox in MATLAB. The identified fluorescent components were compared with previously reported components in the literature to infer their possible sources and characteristics.

Additionally, various FDOM indices, such as the humification index (HIX), biological index (BIX), peak A, and fluorescence index (FI), were used to evaluate the optical properties of the samples. UV-visible absorbance indices were also calculated, such as spectral slope ratio (SR) and specific ultraviolet absorbance at 254 nm (SUVA). These indices provided insights into the humic substance content, autotrophic productivity, recalcitrant and labile DOM, terrestrial and microbial sources of the DOM pool, molecular weight material, and aromatic content of the samples.

2.6. Figure out the influence of filter pore sizes and incubation containers

A 50-day degradation experiment was performed to determine the impact of different incubation containers on the final experimental outcomes. Water samples were stored in a single 1L bottle or separate 50 mL vials for incubation. To minimize errors and enhance the reliability of the experimental results, two filter sizes and two types of samples—river water from the lower Arakawa River and seawater from the near-shore area—were used. This experimental design is detailed in Table 2.5.

Table 2.4 Experiments Design for figuring out the influence of incubation container

Near-shore Area (Seawater)	Arakawa River water
0.45 μm and 50ml vials	0.45 μm and 50ml vials

0.45 µm and 1L bottle	0.45 µm and 1L bottle
0.7 µm and 50ml vials	0.7 µm and 50ml vials
0.7 µm and 1L bottle	0.7 µm and 1L bottle

3. Results

3.1. Sampling arrangements and information

The table provides detailed data on various parameters measured at different sampling points across multiple years, primarily focusing on 2022 and 2023. Each row corresponds to a specific sampling event, identified by the name of the site, the year, and the nature of the sampling (e.g., inflow, outflow, typhoon events). The columns include DIC (Dissolved Inorganic Carbon) measurements, salinity, TA (Total Alkalinity), and pH levels, essential indicators of water quality and chemical composition.

The data reveals a range of conditions across different locations and times. For instance, the Arakawa STP May inflow 2023 shows a high DIC of 2947.55 μmol/L, salinity of 0.28 PSU, TA of 2611.71 μmol/kg, and a pH of 6.764. In contrast, the Edogawa August outflow in 2023 displays significantly different values, with a DIC of 1181.87 μmol/L, salinity of 1.19 PSU, TA of 1165.32 μmol/kg, and a pH of 7.474. These variations highlight the dynamic nature of water quality influenced by factors such as freshwater inputs, tidal mixing, and seasonal changes.

Table 3.1 The info on sampling points

Sample Name	Year	DIC	Salinity	TA	pH
Arakawa STP May Inflow	2023	2947.55	0.28	2611.71	6.764
Arakawa STP May Outflow	2023	1502.7	0.32	1212.39	6.773
Arakawa STP August Inflow	2023	5442.82	0.32	4078.51	6.674
Arakawa STP August Outflow	2023	1556.82	0.39	1299.45	6.85
Edogawa STP East August Outflow	2023	1690.2	0.31	1525.86	7.021
Edogawa STP August Inflow	2023	6854.72	0.46	5120.46	6.326
Edogawa STP 1-8 August Outflow	2023	1317.94	0.35	987.92	6.677
Arakawa August Typhoon	2023	1146.62	0.36	1116.15	7.312
Edogawa August Typhoon	2023	760	0.13	706.48	7.07
Arakawa September Typhoon	2023	1002.45	0.32	948.84	7.192
Edogawa September Typhoon	2023	921.61	0.23	895	7.212
Arakawa May	2023	1452.24	7.78	1318.8	7.075
Arakawa June	2023	1242.78	0.34	1212.36	7.289
Arakawa July	2023	1442.26	3.24	1381.91	7.479
Arakawa August	2023	1394.38	3.51	1304.41	7.326
Arakawa October	2023	1922.17	24.07	2012.04	7.789
Edogawa June	2023	660.11	0.12	598.88	7.012
Edogawa July	2023	1219.29	1.2	1194.67	7.554
Edogawa August	2023	1221.87	1.9	1165.23	7.474
Edogawa October	2023	3672.88	18.81	5263.31	8.643
Arakawa STP October Inflow	2022	3668.97	0.38	3191.42	6.65
Arakawa STP October Outflow	2022	2127.21	2.44	1795.98	7.013
Arakawa STP February Inflow	2023	3369.93	0.45	3094.55	6.802
Arakawa STP February Outflow	2023	1897.55	10.46	1617.28	6.801
Edogawa STP December Inflow	2022	3785.45	0.37	3526.77	7.272

Edogawa STP 1-8 December Outflow	2022	1332.27	0.33	1009.08	6.678
Edogawa STP December East Outflow	2022	1638.66	0.33	1526.06	7.098
Edogawa STP April Inflow	2023	5801	0.48	4782.94	6.582
Edogawa STP 1-8 April Outflow	2023	1066.7	0.32	727.61	6.559
Edogawa STP East April Outflow	2023	1624.5	0.52	1454.87	6.998

Typhoon events are notably marked in the data, such as the Arakawa Typhoon events in August and September 2023. Four samples were specifically marked with the word "typhoon." These samples were collected within 12 hours after a typhoon passed through Tokyo Bay and the lower reaches of the Edogawa and Arakawa Rivers. These collections aimed to study the impact of special events like typhoons on the environment. By analyzing these samples, it is possible to understand how the precipitation, wind, and other environmental changes brought by typhoons affect water quality parameters. Significant changes in water chemistry are observed during these periods, likely due to increased runoff and mixing caused by heavy rainfall and storm surges. For example, the Arakawa August Typhoon 2023 recorded a DIC of 1146.62 μmol/L, salinity of 0.13 PSU, TA of 1118.31 μmol/kg, and a pH of 7.095. These values are markedly different from the more stable conditions observed during non-typhoon periods.

The data also reveal seasonal patterns, with measurements from different months showing distinct trends. For instance, the Arakawa July 2023 sample shows a DIC of 1442.26 μmol/L, salinity of 2.34 PSU, TA of 1318.91 μmol/kg, and a pH of 7.479, reflecting the seasonal influence on water quality parameters. Similarly, samples from Edogawa in various months provide a comprehensive view of how water quality changes over time.

3.2. Substance classification and identification (FDOM)

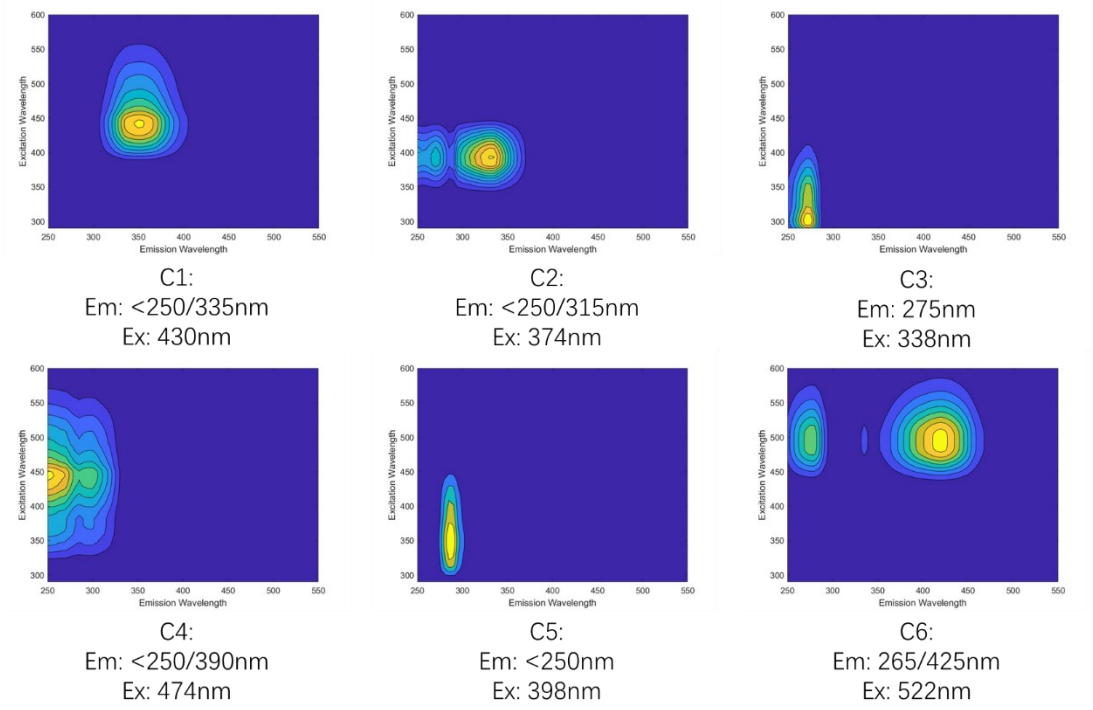

Figure 3.1 EEMs of C1-C6

Table 3.2 Definition of C1-C6

Component	Characterization	Excitation (nm)	Emission (nm)
C1	Humic-like substance, Sewage derived substance	<250 (335)	430
C2	Marine humic-like substance, Microbial humic-like substance	315 (<250)	374
C3	Tryptophan-like substance	275	338
C4	Humic-like substance	<250 (390)	474
C5	Humic-like substance	<250	398
C6	Photodegradation-like substance, Terrestrial humic-like substance	425 (265)	522

FDOM is the portion of dissolved organic matter that exhibits fluorescence in aquatic environments. This fluorescence property allows for detailed analysis using EEMS techniques. In this research, after analyzing the EEMS spectra, we obtained FDOM images and decomposed them into six components: C1, C2, C3, C4, C5, and C6. This decomposition is typically performed using parallel factor analysis (PARAFAC), a multivariate statistical technique that helps identify and quantify independent fluorescent components within complex mixtures. PARAFAC modeling allows for a more detailed understanding of the sources, composition, and transformations of FDOM in natural and engineered systems.

Component C1 is characterized by its excitation peaks below 250 nm and a secondary peak at 335 nm, emitting at 430 nm. This component is identified as a humic-like substance, typically originating from decaying organic matter and sewage. Studies like Stedmon and Markager (2005a) and Murphy et

al. (2011) have found similar fluorophores, specifically C4 and G1, respectively, indicating that C1 is a significant marker of natural and anthropogenic organic matter in aquatic environments [31, 33].

Component C2 shows excitation at 315 nm, with a sub-peak below 250 nm, and emits at 374 nm. It is characterized as a marine humic-like substance, which suggests it originates from marine organisms. Additionally, it exhibits properties of microbial humic-like substances, pointing to a dual origin from marine biological activity and microbial processes. This dual characterization is supported by similar findings in studies like Peak M identified by Coble (1996) and the fluorophore reported by Cory and MaKnight (2005), confirming the presence of marine and microbial humic-like substances in the studied samples [29, 30].

Component C3, with an excitation peak at 275 nm and an emission peak at 338 nm, is identified as a tryptophan-like substance. Tryptophan is an amino acid commonly found in proteins, and its presence in water samples often indicates biological activity, particularly from proteins and peptides. The similarity of this component to Peak T identified in Coble (1996) further supports its identification as a biological indicator, reflecting the contribution of proteinaceous material in the water.

Component C4 exhibits excitation peaks below 250 and 390 nm, with an emission peak at 474 nm. This component is characterized as a humic-like substance, similar to those described by Peak A in Coble (1996) and C1 in Stedmon and Markager (2005b). The humic-like nature of this component suggests it originates from the degradation of terrestrial and aquatic organic material [32].

Component C5 has an excitation peak below 250 nm and emits at 398 nm, indicating it is a humic-like substance. This component is comparable to Peak A found in Coble (1996) and C2 in Stedmon and Markager (2005b). The consistent identification of humic-like substances across various studies reinforces the understanding that Component C5 originates from the breakdown of organic matter [29, 32].

Component C6 is notable for its excitation peaks at 425 nm and 265 nm, with an emission peak at 522 nm. This component is characterized as a photodegradation-like substance and a terrestrial humic-like substance. The presence of this component suggests that it results from the photodegradation of organic material, which is likely influenced by sunlight exposure, as described by C7 in Stedmon and Markager (2005b) [32].

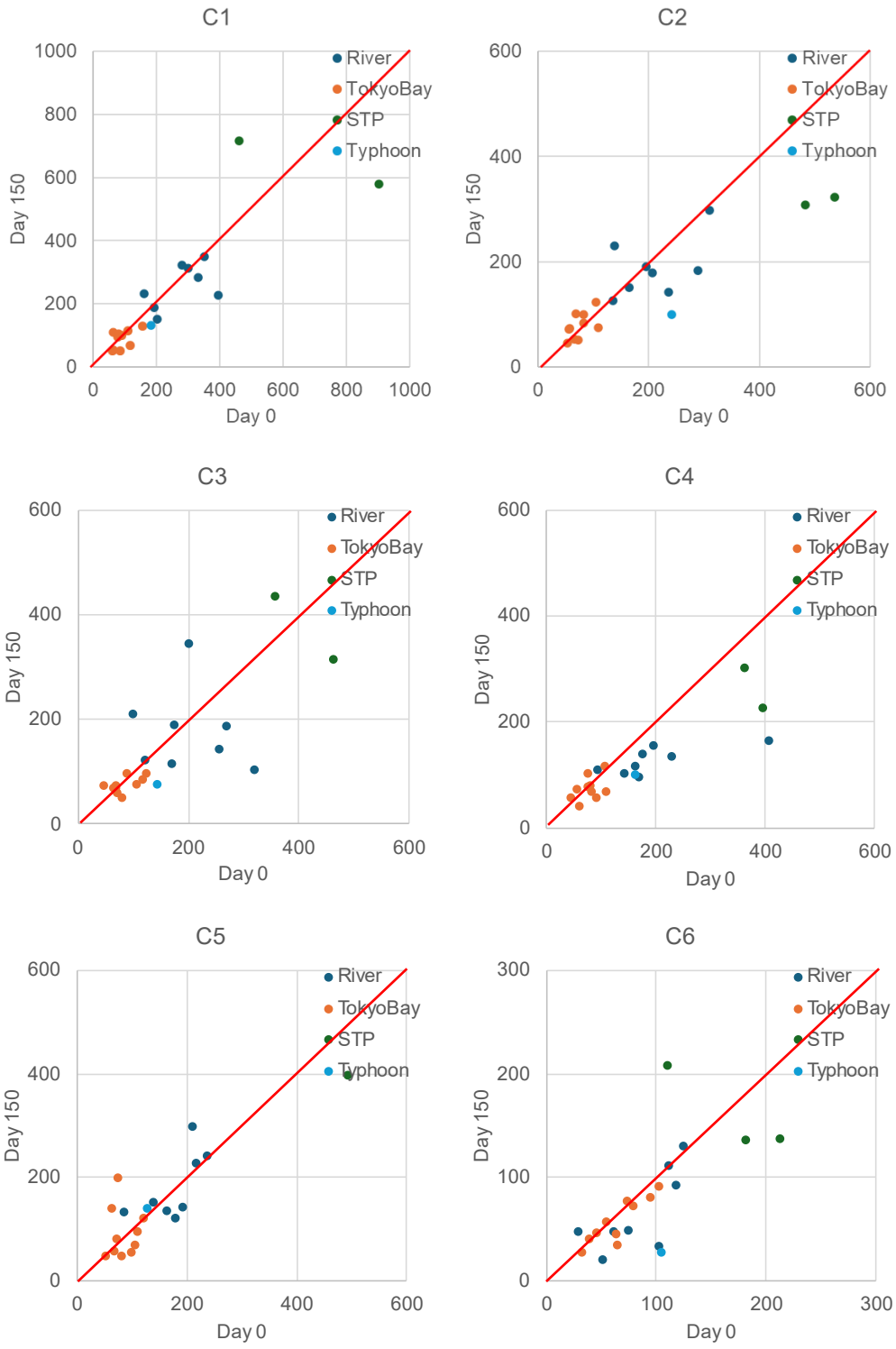

Figure 3.2 Results of Remained C1-C6

Those figures compare the spectral characteristics of a water sample by analyzing the ratio of peak intensities observed on Day 0 and Day 150. These peak intensities are derived from fluorescence spectroscopy data, which measures the emitted light from a sample after it has been excited by a specific wavelength. The positions and intensities of these peaks correspond to the presence and concentration of

various fluorescent compounds in the sample. By comparing these peaks over time, researchers can assess changes in the chemical composition of the water, such as the degradation or formation of compounds. The y = x（1:1） line indicates no change in peak intensity, signifying that the concentration of the fluorescent compounds has remained constant. Data points above this line suggest an increase in peak intensity on Day 150, possibly due to the accumulation of substances or the formation of new fluorescent compounds. Conversely, data points below the line indicate a decrease in peak intensity, which might result from the degradation of fluorescent substances and a reduction in their concentration.

The graph for C1 shows most data points clustering closely along the 1:1 line, indicating very little change in concentration from Day 0 to Day 150. This suggests that C1 is a stable substance with minimal degradation over the observed period. C1 is associated with humic-like substances primarily derived from sewage treatment plant (STP) effluents. Its biological recalcitrance means it resists decomposition, which is reflected in the stability observed in the graph.

The graph for C2 shows data points clustering near but predominantly below the 1:1 line, indicating a decrease in concentration from Day 0 to Day 150. This trend suggests that C2 undergoes some degree of degradation over time. C2 is a marine humic-like substance produced by microbial degradation in terrestrial and aquatic environments. Despite being biologically recalcitrant, the graph demonstrates that C2 does undergo some degradation, though slowly and to a limited extent.

The graph for C3 displays a scattered distribution of data points, with several significantly below the 1:1 line, indicating a reduction in concentration from Day 0 to Day 150. However, some points are above the line, suggesting an increase in concentration in some cases. This variability indicates different rates of degradation and possible additional sources contributing to C3 levels. C3 is associated with protein-like materials and can be produced by phytoplankton, microbial metabolism, domestic wastewater, and STP effluents. The presence of points above the line suggests that new sources or transformations might contribute to the observed concentrations.

The graph for C4 shows data points below the 1:1 line, indicating a moderate reduction in concentration from Day 0 to Day 150. The points are more tightly clustered, suggesting a consistent sample degradation rate. C4 is a humic-like substance, similar to C1 and C2, but exhibits slightly different degradation properties. It is semi-recalcitrant, meaning it undergoes some biological breakdown over time. The graph indicates that while C4 resists degradation, it is less stable than C1 and C2.

The graph for C5 shows data points closely aligning with the 1:1 line, indicating very little change in concentration between Day 0 and Day 150. This suggests that C5 is a stable substance with minimal degradation over the observed period. C5 is believed to originate from andosols widely distributed in the bay's watershed, with higher fluorescence intensity observed at the lower station of the Arakawa River. The graph indicates that additional sources, such as groundwater inflow or terrestrial inputs, influence C5.

The graph for C6 shows most data points clustering tightly along the 1:1 line, indicating very little change in concentration between Day 0 and Day 150. The close alignment of points with the line signifies high stability and minimal degradation over time. C6 is associated with humic-like characteristics and is highly recalcitrant. The graph demonstrates that C6 remains stable and does not undergo significant biological or chemical degradation within 150 days, maintaining consistent behavior.

3.3. DOC degradation in rivers and sewage treatment plants

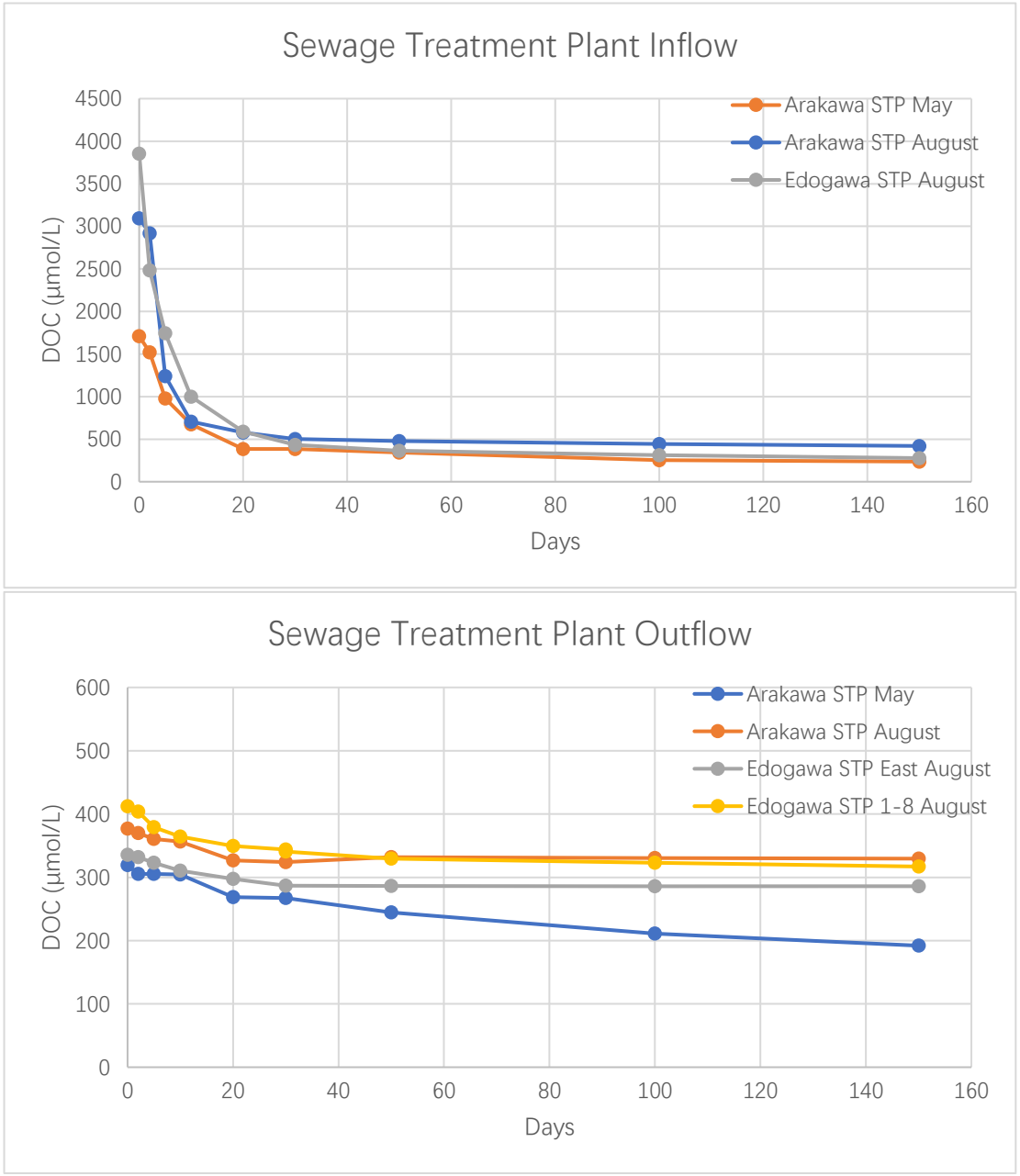

Figure 3.3 Degradation results of Kasai and Edo STPs

The inflow data from wastewater treatment plants represent the domestic sewage and other types of wastewater flowing into the treatment facility from urban areas. The outflow data represent the treated water directly discharged into the two rivers after treatment at the wastewater treatment plant. It is

important to note that water with high concentrations of DOC and low molecular weight LDOC is not directly discharged into rivers and seas.

The provided image contains two line graphs illustrating the changes in DOC concentrations over time for sewage inflow and outflow at an STP. The Sewage Inflow plots DOC concentrations on the y-axis, ranging from 0 to 3500 μmol/L, against days on the x-axis, ranging from 0 to 150. Three different colored lines represent different measurement points or types of inflow: orange for the Arakawa STP inflow in May, blue for the Arakawa STP inflow in August, and gray for the Edogawa STP inflow in August. All three lines show a steep decline in DOC concentrations within the first 20 days. After this steep decline, the DOC concentrations level off and stabilize, remaining relatively constant from around 50 to 150 days. Initially, the DOC concentration is highest for the Arakawa STP inflow in August, followed by the Arakawa STP inflow in May and Edogawa STP inflow in August. However, they all converge to similar levels below 500 μmol/L after 40 days.

The second graph plots DOC concentrations on the y-axis, ranging from 0 to 600 μmol/L, against days on the x-axis, ranging from 0 to 160. Again, four different colored lines represent different measurement points or types of outflow: blue for the Arakawa STP outflow in May, orange for the Arakawa STP outflow in May, gray for the Edogawa STP East outflow in August, and yellow for the Edogawa STP 1-8 outflow in August. The Arakawa and Edogawa outflows show an initial decrease in DOC concentration in the first 40 days, followed by stabilization. However, the Arakawa STP outflow in August shows a different trend, with DOC concentration increasing gradually from day 40 onwards, intersecting and eventually surpassing the Edogawa STP 1-8 outflow. Around days 100 to 150, all lines show some fluctuations but generally remain within a range of 300 to 400 μmol/L for the Arakawa STP outflow in August and the Edogawa STP 1-8 outflow and around 200 to 300 μmol/L for the Edogawa STP East outflow in August and Arakawa STP outflow in May.

Together, these two graphs provide insights into the efficiency and dynamics of DOC removal at the STP. The inflow graph demonstrates a rapid reduction in DOC concentrations early in incubation. However, the effluent plot shows that the initial DOC concentration decreased. However, the initial concentration and the rate of decline were lower than in the sewage degradation experiment. This indicates that most dissolved organic carbon compounds were removed after treatment at the sewage treatment plant.

3.4. DOC degradation

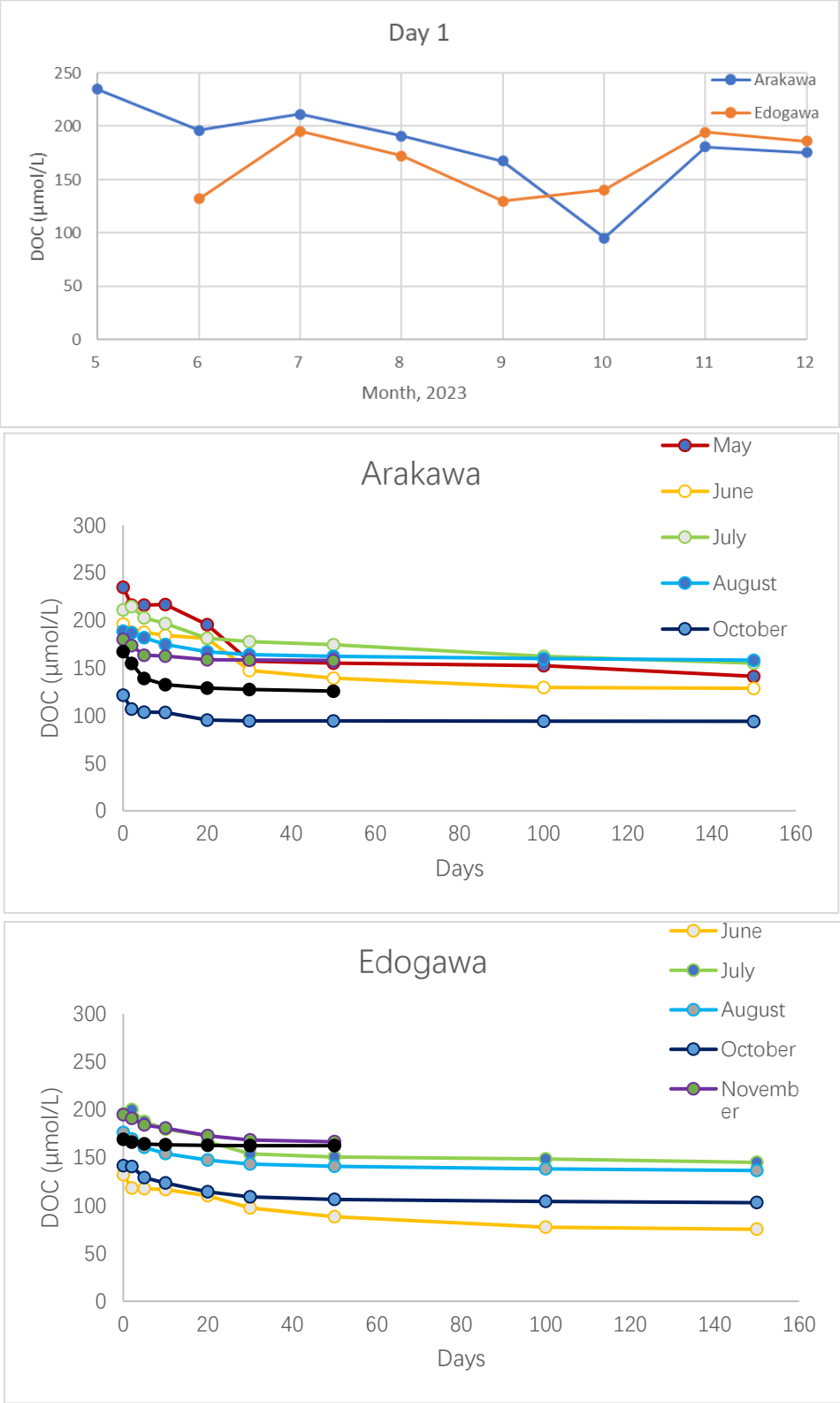

Figure 3.4 DOC degradation

The first graph presents the DOC (Dissolved Organic Carbon) concentrations measured in the Arakawa and Edogawa rivers over several months in 2023, specifically from May to December. The blue line represents the DOC concentrations in the Arakawa River, while the orange line represents the Edogawa River. This visual comparison highlights the temporal variations and differences in DOC levels between the two rivers throughout the study period. In May, the Arakawa River shows the highest DOC concentration, reaching approximately 250 μmol/L, slightly decreasing in June. Both rivers exhibit some fluctuations in DOC concentrations over the subsequent months, reflecting the dynamic nature of organic carbon inputs and processing within these aquatic systems. From July to September, the DOC levels in both rivers follow a relatively stable trend, with slight increases and decreases but generally maintaining a consistent range. The Arakawa River shows a minor peak in July, while the Edogawa River's DOC levels remain more stable. However, a noticeable decline in DOC concentration occurs in October for both rivers, with the Arakawa River reaching its lowest point, just above 100 μmol/L, and the Edogawa River also experiencing a significant drop. In November and December, the DOC concentrations in both rivers increase again, suggesting a seasonal influence on organic carbon dynamics. The Arakawa River's DOC levels rise more sharply than the Edogawa River, indicating a potential increase in organic matter inputs or changes in riverine processing of organic carbon as the year progresses.

The second graph shows the Arakawa River's DOC concentration over time. The y-axis represents DOC concentration in μmol/L, ranging from 0 to 300, while the x-axis represents time in days, ranging from 0 to 150. Multiple colored lines represent different months of the year, including May (red), June (yellow), July (light blue), August (dark blue), October (purple), November (pink), and December (cyan). Initially, all lines start at higher DOC concentrations, with the highest around 250 μmol/L in May. Over time, there is a noticeable decrease in DOC concentration, especially within the first 40 days. After this initial decline, the concentrations tend to stabilize, gradually decreasing until day 150. The sampling point in May is downstream of the sewage treatment plant, so it is not used as seasonal data. However, it can be clearly seen that the river water has improved significantly after passing through the sewage treatment plant.

The third graph depicts the DOC concentration over time for the Edogawa River. Like the first graph, the y-axis represents DOC concentration in μmol/L, ranging from 0 to 300, and the x-axis represents time in days, ranging from 0 to 150. Different colored lines represent different months: June (yellow), July (light blue), August (dark blue), October (purple), November (pink), and December (cyan). The initial DOC concentrations are slightly lower than in the Arakawa River, with values starting below 200 μmol/L. The graph shows a decline in DOC concentration within the first 30 days, followed by a stabilization and gradual decrease towards day 150. The yellow line representing June shows a more pronounced decline than the other months.

The second and third graphs show a similar trend of decreasing DOC concentrations over time, with the most significant reductions occurring within the first 50 days. This indicates an initial phase of rapid DOC degradation or removal. After this period, the DOC levels tend to stabilize and decrease more gradually. The primary difference between the two graphs is the initial DOC concentration levels, with the Arakawa River having higher starting concentrations than the Edogawa River. Additionally, the patterns of decline and stabilization vary slightly between the two rivers, with the Edogawa River

showing a more uniform decrease across the months. In contrast, the Arakawa River exhibits more variability in the initial decline phase.

3.5. RDOC concentration during typhoon

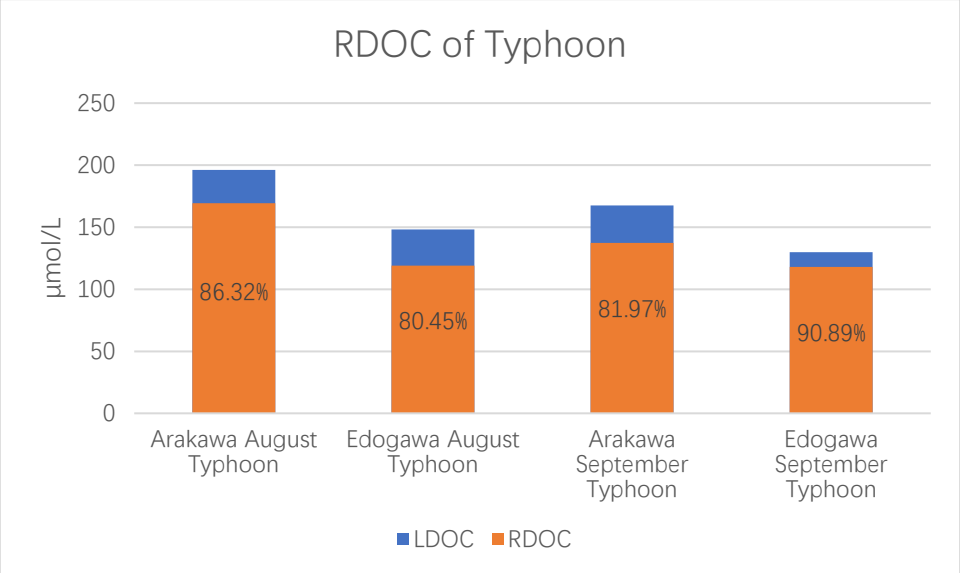

Figure 3.5 RDOC of Typhoon

In previous studies, the total organic carbon (TOC) measured on day 0 of the water samples was considered the total DOC. After a degradation experiment lasting over 150 days, the TOC measured was considered the RDOC. The difference between the DOC content and the RDOC content represents the LDOC.

This figure presents a bar chart comparing RDOC concentrations during typhoon events at Arakawa and Edogawa. The data is depicted for two distinct time points: Day 0 and Day 150, with RDOC concentration measured in μmol/L.

During the August typhoon at Arakawa, the RDOC concentration on Day 0 was approximately 210 μmol/L, but it decreased to around 180 μmol/L by Day 150. The ratio of Day 150 to Day 0 is approximately 0.86, indicating a reduction in RDOC concentration over time.

At Edogawa during the August typhoon, the RDOC concentration starts at around 180 μmol/L on Day 0 and reduces to approximately 145 μmol/L by Day 150. The ratio of Day 150 to Day 0 is approximately 0.80, showing a decrease in RDOC levels over the 150 days.

During the September typhoon at Arakawa, the initial RDOC concentration on Day 0 was about 200 μmol/L, which decreased to roughly 160 μmol/L by Day 150. The ratio of Day 150 to Day 0 is approximately 0.82, reflecting a decline in RDOC concentration over time.

At Edogawa during the September typhoon, the RDOC concentration on Day 0 was approximately 160 μmol/L, which was reduced to about 135 μmol/L by Day 150. The ratio of Day 150 to Day 0 is approximately 0.84, indicating a reduction in RDOC concentration over the observed period.

3.6. RDOC concentration by months

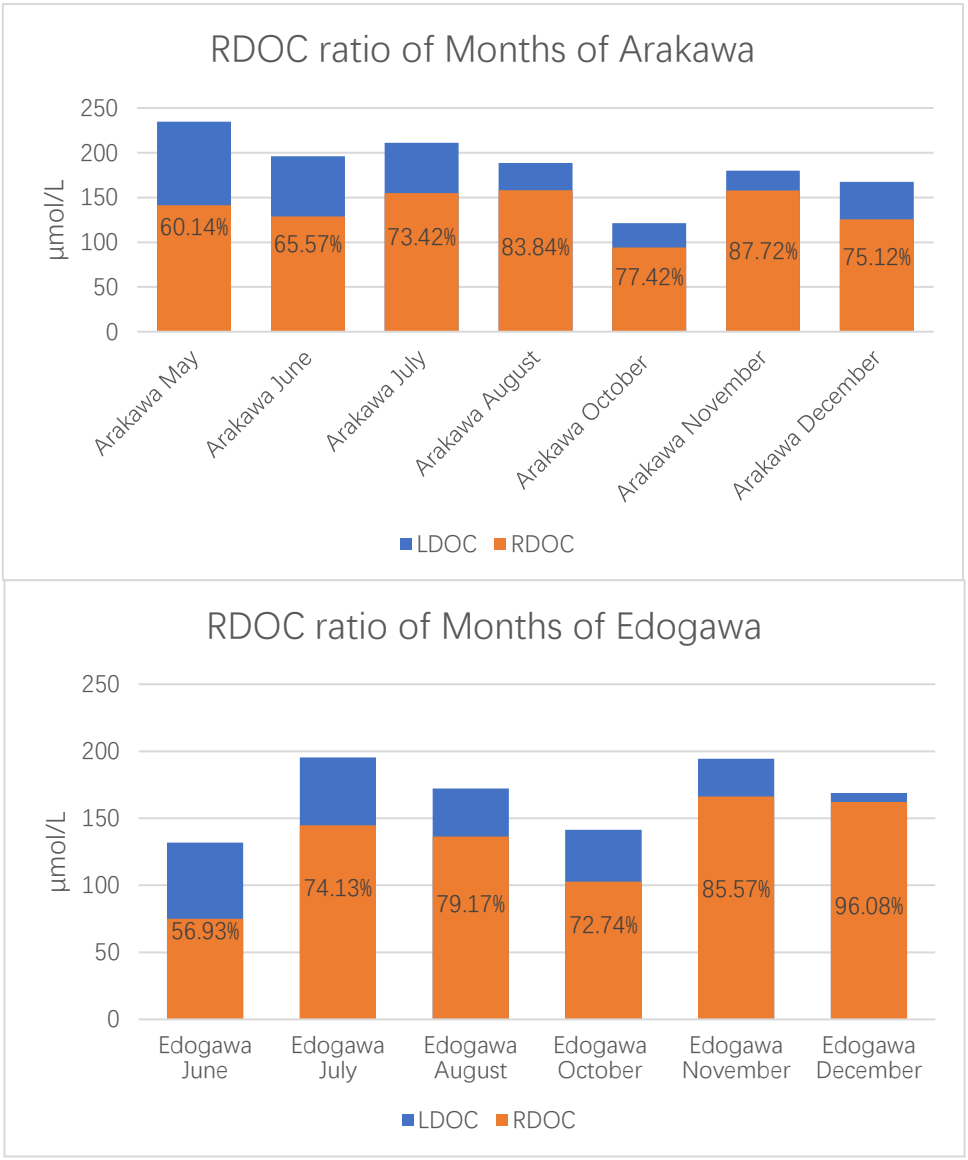

Figure 3.6 RDOC of Months

This figure consists of two bar charts showing RDOC concentrations across different months at Arakawa and Edogawa. The data is presented for two-time points: Day 0 and Day 150, with RDOC concentrations measured in micromoles per liter (μmol/L).

In May, Arakawa's RDOC concentration on Day 0 is approximately 210 μmol/L, which decreases to around 125 μmol/L by Day 150. The ratio of Day 150 to Day 0 is approximately 0.60, indicating a

significant reduction in RDOC concentration over time. In June, the RDOC concentration starts at around 200 μmol/L on Day 0 and reduces to approximately 135 μmol/L by Day 150. The ratio of Day 150 to Day 0 is approximately 0.66, showing a decrease in RDOC levels over the 150 days. In July, the RDOC concentration on Day 0 is about 190 μmol/L, which decreases to roughly 140 μmol/L by Day 150. The ratio of Day 150 to Day 0 is approximately 0.73, reflecting a decline in RDOC concentration over time. In August, the initial RDOC concentration is around 190 μmol/L on Day 0, which decreases to approximately 160 μmol/L by Day 150. The ratio of Day 150 to Day 0 is approximately 0.84. In October, the RDOC concentration starts at about 180 μmol/L on Day 0 and decreases to around 140 μmol/L by Day 150. The ratio of Day 150 to Day 0 is approximately 0.77. In November, the RDOC concentration is approximately 180 μmol/L on Day 0, which decreases to around 155 μmol/L by Day 150. The ratio of Day 150 to Day 0 is approximately 0.87. In December, the RDOC concentration on Day 0 is around 180 μmol/L, which decreases to approximately 135 μmol/L by Day 150. The ratio of Day 150 to Day 0 is approximately 0.75.

For Edogawa in June, the RDOC concentration on Day 0 is approximately 155 μmol/L, which decreases to around 85 μmol/L by Day 150. The ratio of Day 150 to Day 0 is approximately 0.56. In July, the RDOC concentration starts at about 200 μmol/L on Day 0 and decreases to approximately 145 μmol/L by Day 150. The ratio of Day 150 to Day 0 is approximately 0.74. In August, the initial RDOC concentration is around 190 μmol/L on Day 0, which decreases to approximately 150 μmol/L by Day 150. The ratio of Day 150 to Day 0 is approximately 0.79. In October, the RDOC concentration is about 170 μmol/L on Day 0, which decreases to roughly 125 μmol/L by Day 150. The ratio of Day 150 to Day 0 is approximately 0.73. In November, the RDOC concentration is around 170 μmol/L on Day 0, which decreases to approximately 145 μmol/L by Day 150. The ratio of Day 150 to Day 0 is approximately 0.86. In December, the RDOC concentration starts at about 170 μmol/L on Day 0 and decreases to roughly 165 μmol/L by Day 150. The ratio of Day 150 to Day 0 is approximately 0.96.

3.7. RDOC concentration of STP

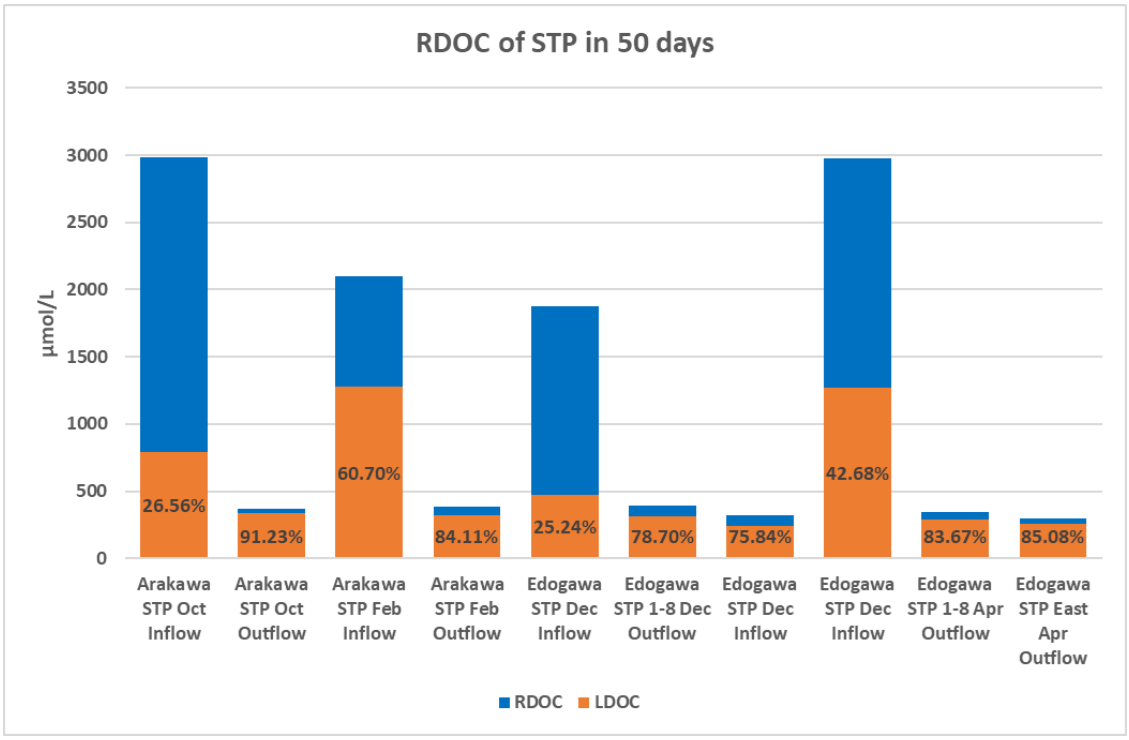

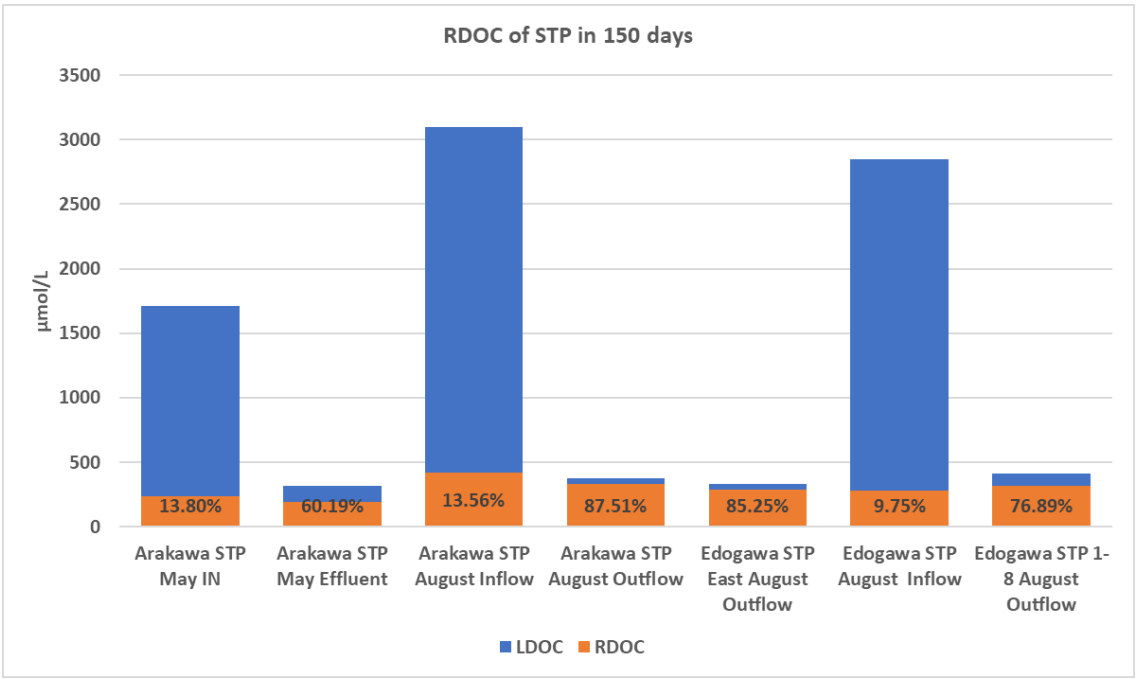

Figure 3.7 RDOC of different STP samples.

The bar chart illustrates the concentrations of RDOC and LDOC in samples taken from the Kasai and Edogawa STPs over a period of 50 days, encompassing different sampling months in October and December 2022 and February and April 2023. The bars are color-coded to differentiate between RDOC and LDOC and the periods of the measurements.

The chart shows that for the Kasai STP inflow samples, there is a substantial amount of DOC, with RDOC in October and December 2022 (dark blue) and February and April 2023 (dark green) making up a significant portion of the total DOC concentration. The LDOC for the same periods (light blue and light green) also contributes notably to the total DOC but to a lesser extent than RDOC. This pattern suggests that the inflow to the Kasai STP contains a considerable amount of persistent organic carbon that is resistant to decomposition, along with a smaller proportion of readily decomposable organic carbon.

In contrast, the Kasai STP outflow samples show a marked reduction in both RDOC and LDOC concentrations. This decrease indicates that the treatment processes at the STP effectively reduce the levels of both types of DOC before the water is discharged. However, the reduction is more pronounced for RDOC, reflecting the challenge of completely removing recalcitrant carbon compounds through standard treatment processes.

The Edogawa STP inflow samples display a similar pattern to the Kasai STP, with high levels of RDOC and LDOC. The inflow samples from February and April 2023 (dark green and light green) show particularly high concentrations of DOC, surpassing 2500 μmol/L, indicating a significant input of organic carbon during this period. The outflow samples from the Edogawa STP, however, show a noticeable decrease in both RDOC and LDOC, although not as pronounced as in the Kasai STP. This suggests that while the Edogawa STP effectively reduces DOC levels, some recalcitrant organic carbon remains in the treated water.

The second bar graph illustrates the ratio of RDOC concentrations from Day 150 to Day 0 across various sampling points, events, and months for the Arakawa and Edogawa rivers. The y-axis represents the ratio of RDOC concentrations (Day150/Day0), indicating the proportion of RDOC remaining after 150 days relative to the initial concentration. The x-axis lists different sampling points, including various months, inflow and outflow points, and river typhoon events.

For the Arakawa River, the ratios for different sampling points are as follows: the STP May Inflow has a ratio of approximately 0.13, indicating a significant reduction in RDOC, while the STP May Effluent shows a ratio of around 0.60, showing a moderate reduction in RDOC. The STP August Inflow has a ratio of approximately 0.13, indicating a significant reduction in RDOC, whereas the STP August Outflow shows a ratio of about 0.87, indicating higher persistence of RDOC. The ratios for typhoon events also reflect significant persistence, with the August Typhoon at approximately 0.86 and the September Typhoon at about 0.81. Monthly measurements for the Arakawa River indicate the following ratios: May at approximately 0.60, June at around 0.65, July at about 0.73, August at approximately 0.83, October at around 0.77, November at about 0.87, and December at approximately 0.75.

For the Edogawa River, the STP August Inflow shows an anomaly with a very high ratio of approximately 9.74, while the STP August Outflow (East) has a ratio of about 0.85, indicating a high persistence of RDOC. The STP 1-8 August Outflow has a ratio of approximately 0.76. Typhoon events in August and September have ratios of around 0.80 and about 0.90, respectively, indicating high persistence of RDOC. Monthly measurements for the Edogawa River show the following ratios: June at approximately 0.56, July at around 0.74, August at about 0.79, October at approximately 0.72, November at around 0.85, and December at about 0.96.

Those two graphs reveal that RDOC concentrations generally remain relatively stable over 50 to 150 days, with ratios typically ranging from 0.6 to 0.9 for most sampling points. However, significant degradation is observed in specific inflow and effluent points, particularly in May for the Arakawa River. The higher ratios during typhoon events indicate that these events may contribute to the persistence of RDOC in the water.

3.8. Spatial distribution of water quality parameters in Tokyo Bay

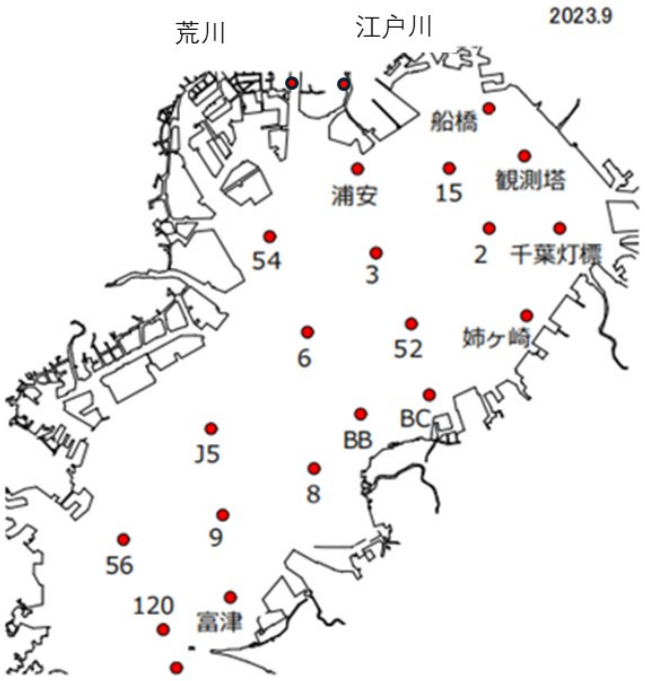

Figure 3.8 Sampling point of the Tokyo Bay experiment

Table 3.3 Tokyo Bay water quality parameters

	DOC(μ mol/L) Day0	Water temp	Salinity	PH	Density (kg/m3)	Chl-a (μg/L)
富津	147.3090606	26.774	30.432	8.192	1019.353	0.8927
120	144.1611157	27.634	31.462	8.236	1019.854	1.776

56	170.9616986	27.334	30.145	8.28	1018.961	1.589
J5	191.1427977	27.567	28.407	8.334	1017.583	2.056
6	187.8226478	28.237	27.559	8.452	1016.735	2.056
3	189.019	28.193	26.625	8.485	1016.046	2.243
54	198.7614488	28.269	24.903	8.512	1014.733	5.094
Urayasu	249.8751041	28.509	24.918	8.78	1014.673	42.402
15	262.7810158	28.549	24.655	8.658	1014.463	12.602
Funabashi	209.5753539	29.666	23.672	8.76	1013.369	30.291
Off Kemigawa Observatory	226.5255145	28.994	24.796	8.537	1014.426	3.801
2	194.4733555	28.751	26.325	8.52	1015.647	2.952
Chiba Light House	189.4462948	29.883	25.477	8.527	1014.644	2.477
Anegasaki	181.4425479	28.645	26.988	8.476	1016.177	2.672
52	184.325562	29.227	27.479	8.47	1016.354	2.531
BC	166.5383014	28.253	28.729	8.308	1017.606	2.017
BB	158.7635304	28.338	29.517	8.222	1018.177	1.698
8	145.5141549	27.921	30.823	8.273	1019.283	2.157
9	138.3430475	28.254	30.14	8.38	1018.664	3.51
Arakawa River	167.4900546		3.24	7.479		
Edogawa River	129.9000833		1.2	7.554		

The provided figures include a map showing sampling locations and a table detailing various parameters measured at these sites. The map displays numerous red dots representing different sampling sites across the study area, each marked with unique identifiers such as numbers or letters (e.g., 54, 15, J5, BB). The names of two rivers, 荒川 (Arakawa) and 江戸川 (Edogawa), are labeled, indicating the primary

freshwater inflow points into the area. These sampling sites are strategically distributed throughout the region, covering both northern and southern parts, ensuring comprehensive spatial coverage for the study.

The accompanying table provides detailed measurements for various parameters at each sampling site. Each row corresponds to a specific location as marked on the map. The columns include parameters such as depth (in meters), salinity (in Practical Salinity Units, PSU), and other relevant metrics. For example, the depth column indicates the depth at which measurements were taken at each site, providing context for the variations in the data. The salinity column shows the salinity levels at each site, which vary significantly across different locations, reflecting the influence of freshwater inputs and mixing with seawater.

The data presented in the table reveal interesting patterns. Higher salinity levels are generally observed in the southern part of the study area. In comparison, lower salinity levels are noted in the northern regions, likely due to the freshwater inputs from the Arakawa and Edogawa rivers. This pattern is consistent with the spatial distribution of salinity depicted in the earlier figure. By examining these measurements, researchers can gain insights into the hydrodynamic processes and the influence of riverine inputs on the water quality in the study area. These detailed observations are crucial for understanding the environmental conditions and guiding effective management strategies for the aquatic ecosystem.

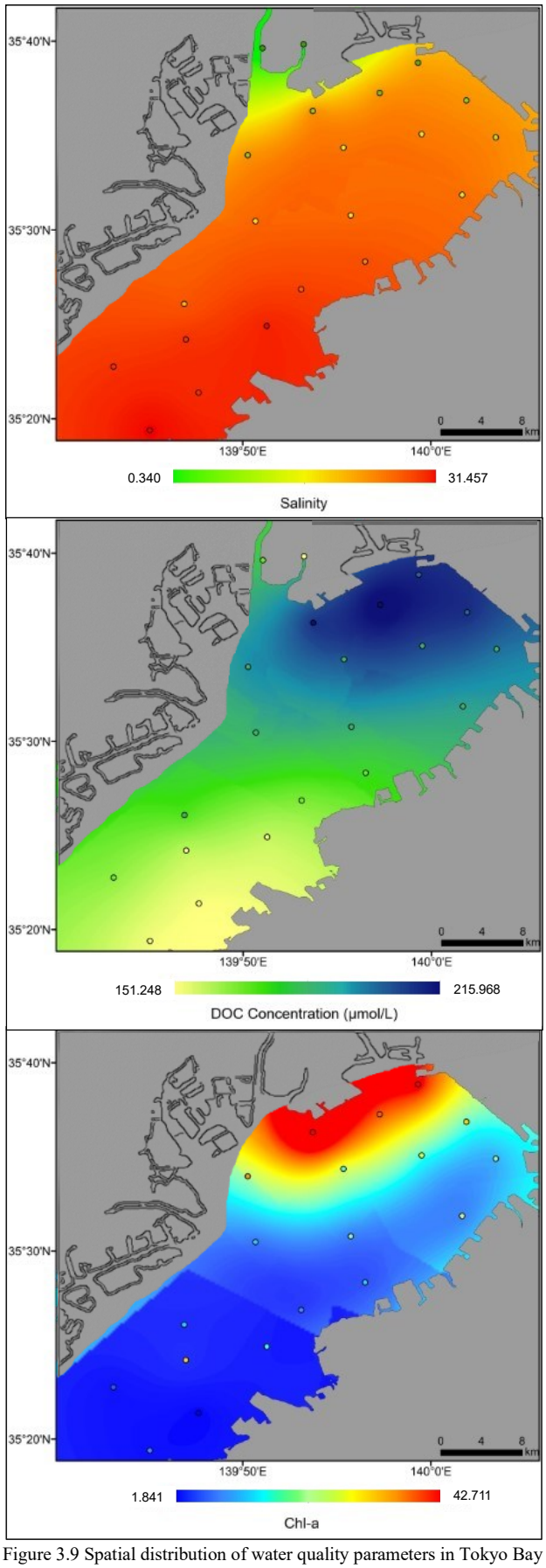

Figure 3.9 Spatial distribution of water quality parameters in Tokyo Bay

The presented figure consists of three maps illustrating the spatial distributions of salinity, DOC concentration, and Chl-a concentration in the study area. In the analysis of Tokyo Bay samples, data from two additional samples taken from the lower reaches of the Arakawa and Edogawa Rivers were included. This integration allows for a comprehensive analysis of the entire upper watershed of Tokyo Bay. The first map shows the salinity distribution, with values ranging from 0.340 to 31.457 PSU (Practical Salinity Units). Higher salinity values are observed in the southern part of the area, indicating more saline conditions. In comparison, lower salinity values are found in the northern regions, likely due to freshwater inputs from rivers and streams.

The second map depicts the distribution of DOC concentrations ranging from 151.248 to 215.968 μmol/L. The highest DOC concentrations are located in the northern parts of the study area, coinciding with regions of lower salinity. This pattern suggests that freshwater inputs, typically rich in organic matter, contribute significantly to the DOC levels in these areas. As the water moves southward, the DOC concentrations decrease, indicating dilution or degradation of organic matter.

The third map presents the Chl-a concentration, ranging from 1.841 to 42.711 μg/L. The highest Chl-a concentrations are found in the northern regions, where nutrient-rich freshwater inputs likely promote phytoplankton growth. This pattern is consistent with lower salinity and higher DOC concentrations, supporting the fact that nutrient availability from freshwater sources enhances primary productivity. The southern part of the study area shows lower Chl-a concentrations, corresponding with higher salinity and lower DOC levels, indicating less favorable conditions for phytoplankton growth.

Overall, the spatial patterns observed in these maps suggest a strong influence of freshwater inputs on the distribution of salinity, DOC, and Chl-a in the study area. The northern regions, characterized by lower salinity and higher DOC and Chl-a concentrations, appear to benefit from nutrient-rich freshwater inflows, promoting phytoplankton blooms and higher primary productivity. In contrast, the southern regions exhibit higher salinity, lower DOC, and lower Chl-a concentrations, reflecting more marine conditions and potentially lower nutrient availability.

3.9. Influence of different pore sizes of filters and incubation containers

Table 3.4 DOC (μmol L-1), LDOC (μmol L-1), RDOC (μmol L-1) at Near-shore areas using different incubation containers

Station	Filter pore size	Container	Sampling date	DOC	LDOC	RDOC
NS Area	0.45μm	50ml vials	Feb. 2023	140.81	47.47	93.34
NS Area	0.7μm	50ml vials	Feb. 2023	148.97	63.92	85.05

NS Area	0.45μm	1L bottle	Feb. 2023	140.81	37.29	103.52
NS Area	0.7μm	1L bottle	Feb. 2023	148.97	65.83	83.14

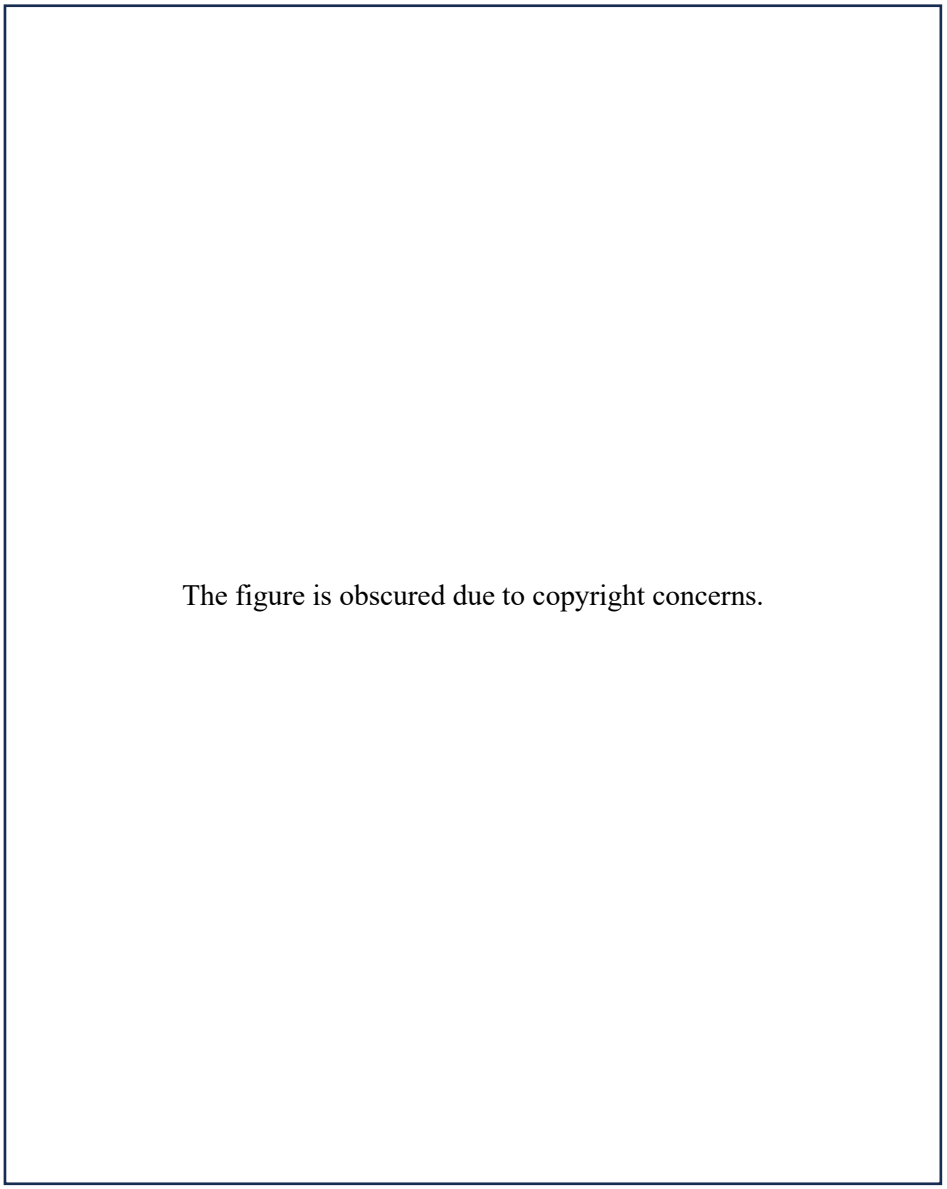

Figure 3.10 Degradation result of different incubation containers

Figure 3.10 illustrates the results of degradation experiments using various incubation methods. For samples from the Near-shore area, regardless of the incubation container, the residual DOC (RDOC) value of the 0.7μm samples after 50 days was consistently lower than that of the 0.45μm samples, as expected. The 0.7μm filtrates contained more bacteria than the 0.45μm filtrates, leading to increased DOC decomposition through microbial activity.

For the 0.7μm samples, the 1-liter container resulted in greater DOC decomposition and a lower RDOC ratio. However, for the 0.45μm samples, the 1-liter container did not significantly impact DOC decomposition, likely due to the lower microbial community composition.

In the 50 ml vials, 30 ml of air space was maintained, whereas in the 1-liter bottles, 300 ml of air space was kept. Assuming that 1 mole of organic carbon mineralized into CO_2 would consume 1 mole of oxygen, these headspaces should have provided adequate oxygen supply for microbial decomposition. Thus, neither container should have experienced oxygen limitations.

However, scientific studies have shown that a larger relative surface area, where water is exposed to air, allows for greater gas exchange, including oxygen, between the water and the atmosphere. This enhanced gas exchange can lead to higher oxygen availability for biological processes, especially for the degradation of organic matter.

This implies that incubation in a 1-liter bottle, which provides a larger relative surface area, should have a higher oxygen concentration, which is one of the contributing factors. Additionally, in this experiment, the 1-liter bottles were shaken before each measurement, whereas the 50 ml vials were rarely shaken because they were independent of each other.

This indicates that the 1-liter bottle condition likely provided better mixing efficiency, with more sufficient oxygen supplementation than the separate vials, resulting in higher DOC decomposition in the 1-liter samples. Both the 50 ml vials and the 1-liter bottles were covered with aluminum foil to prevent light exposure, so there was no difference in light conditions.

Since no nutrients were added during the experiments, the microbial community composition should have been the same for each sampling site. Larger error bars were observed in the 50 ml vial samples. This could be because dispensing into separate vials might have led to slightly different compositions between different vials, resulting in varying DOC degradation conditions.

Table 3.5 DOC (μmol L^{-1}), LDOC (μmol L^{-1}), RDOC (μmol L^{-1})at Near-shore areas using different filter pore sizes

Station	Filter pore size	Sampling date	DOC	LDOC	RDOC
NS Area	0.45μm	May. 2023	156.03	19.05	136.98 (87.8%)
NS Area	0.7μm	May. 2023	149.28	45.21	104.07 (69.7%)
NS Area	1.2μm	May. 2023	155.11	49.51	105.6 (68.1%)
NS Area	1.2-0.7μm	May. 2023	165.2	50.93	114.27 (69.2%)
NS Area	2.7μm	May. 2023	152.46	55.39	97.07 (63.7%)

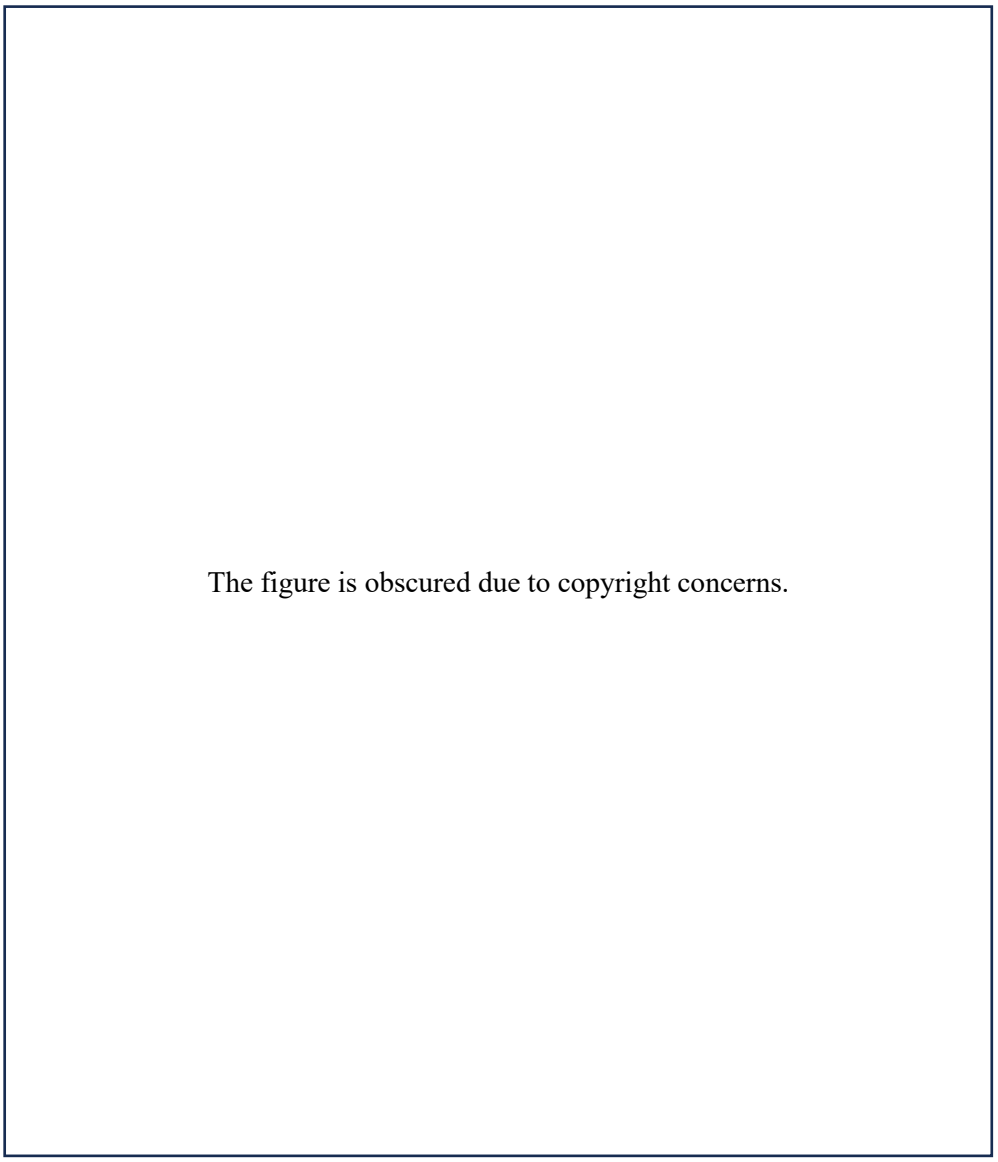

Figure 3.11 degradation result of different filter pore sizes

The pore size of filters determines the extent to which bacteria, which play a crucial role in the degradation process, are retained in the samples. Smaller pore sizes tend to remove more bacteria, potentially limiting their availability for DOC degradation and leading to lower degradation rates. Conversely, filters with larger pore sizes may allow smaller organic molecules to pass through while retaining larger particles, thus influencing the composition of the remaining DOC pool and potentially affecting degradation rates.

Figure 3.11 shows the degradation results from two sampling sites using filters with different pore sizes. A percentage stacked column chart accounted for variations in initial and final DOC values due to different filter sizes (Figure 3.11).

It is evident that 0.45μm filters remove more bacteria than larger filters, leading to an overestimation of the RDOC ratio. The 0.45μm filters should have removed nearly all bacteria from the water. However, degradation rates were still observed. This is because 0.45μm filters were syringe sterile filters that could not be pre-combusted, potentially introducing some bacteria into the samples during filtration. Additionally, DOC might chemically react with the glass bottles, contributing to the observed decrease in DOC.

The RDOC ratios estimated using 0.7μm and 1.2μm filters were similar but lower than those obtained using 0.45μm filters for both samples. This indicates that both 0.7μm and 1.2μm filters allowed more bacteria to pass through, resulting in more DOC decomposition within the same period. However, bacteria with diameters ranging from 0.45 to 0.7μm comprised most of the bacteria within the 0.45 to 1.2μm size range.Denis et al. (2017) found no significant differences between DOM<0.2μm and DOM<0.7μm for bulk scale descriptors, and the distribution of 43 targeted compounds was not impacted at the molecular scale. Assuming the DOC passing through 0.45μm and 0.7μm filters contain the same compounds, the main factor causing the degradation differences is the bacterial community composition.

For near-shore areas, 2.7μm filtrates exhibited much lower RDOC ratios than 1.2μm filtrates, which is consistent with expectations. This indicates that 2.7μm filtrates included more bacteria, resulting in more DOC decomposition over the same period. Dean et al. (2018) conducted similar experiments testing the impact of three different filtration strategies, including 0.2μm, 0.7μm, and unfiltered samples. They found that both bacterial community composition and DOM degradation dynamics were affected by different filter sizes. However, unfiltered samples converged to the common total DOM bio-lability level more slowly than 0.7μm samples, indicating that the dynamics of the two responses were decoupled.

It is suggested that filtration primarily affects bio-lability assays through bacterial abundance and the presence of associated predators. In this research, 2.7μm filtrates included more bacteria and more predators and contained more particulate organic matter. Considering the degradation curve still slightly decreased even on the 50th day (Figure 3.11), a more extended incubation period should be applied to 2.7μm filter samples. The different tendencies observed in the 2.7μm filtrates between the two samples are likely due to differences in bacterial community composition. The container size and

configuration are crucial considerations as they influence factors such as oxygen availability, light penetration, microbial activity, and nutrient availability, all of which impact DOC degradation. Using smaller, separate 50 ml vials can provide a more controlled and confined environment for microbial activity, allowing for better monitoring of the degradation process. Conversely, storing samples in a larger 1-liter bottle may offer a more natural or realistic setting, facilitating interactions between different microbial communities and providing a more representative degradation process.

In the 50 ml vials, 30 ml of air space was maintained, whereas in the 1-liter bottles, 300 ml of air space was kept. Assuming that 1 mole of organic carbon mineralized into CO2 consumes 1 mole of oxygen, these headspaces should provide sufficient oxygen supply for microbial decomposition. Thus, neither container should have experienced oxygen limitations. However, scientific studies have shown that a larger relative surface area, where water is exposed to air, allows for greater gas exchange, including oxygen, between the water and the atmosphere. This enhanced gas exchange can lead to higher oxygen availability for biological processes, especially for the degradation of organic matter. This implies that incubation in a 1-liter bottle, which provides a larger relative surface area, should have a higher oxygen concentration, which is one of the contributing factors. Additionally, in this experiment, the 1-liter bottles were shaken before each measurement, whereas the 50 ml vials were rarely shaken because they were independent of each other. This indicates that the 1-liter bottle condition likely provided better mixing efficiency, with more sufficient oxygen supplementation than the separate vials, resulting in higher DOC decomposition in the 1-liter samples. Both the 50 ml vials and the 1-liter bottles were covered with aluminum foil to prevent light exposure, so there was no difference in light conditions.

Since no nutrients were added during the experiments, the microbial community composition should have been the same for each sampling site. Larger error bars were observed in the 50 ml vial samples. This could be because dispensing into separate vials might have led to slightly different compositions between different vials, resulting in varying DOC degradation conditions.

Through these two steps, my research ultimately chose the 1-liter container and 0.7μm filter paper. Therefore, this section will not be presented in the discussion.

4. Discussion

4.1. DOC degradation

The changes in substance concentrations show differing stability and degradation rates. C1 and C5, with data points near the 1:1 line, are stable and degrade minimally, reflecting their resistant origins like STP effluents .C2, C3, and C4 display varying levels of degradation, mainly below the 1:1 line, indicating breakdown over time. Notably, C3 sometimes increases, suggesting additional sources or transformations, especially from phytoplankton and microbial activity.C1, C5, and C6's stability suggests minimal short-term impact on water quality, though they may accumulate over time. In contrast, C2, C3, and C4's degradation highlights their role in natural pollutant attenuation. The variability in C3 requires further study to understand its sources and degradation conditions.

The study of DOC degradation in the Arakawa and Edogawa rivers and the STPs in these regions reveals significant insights into the biogeochemical processes and treatment efficiencies in urbanized coastal waters. The variability observed in DOC concentrations, salinity, TA, and pH levels across different sampling points and conditions underscores the complex dynamics influencing water quality in these environments. Seasonal and event-based variations, such as those observed during typhoon events, significantly impact the levels of these parameters, reflecting changes in organic matter inputs and microbial activity. This trend aligns with findings from other studies noting higher DOC levels in warmer months due to increased biological activity and organic matter decomposition [34][35].

Seasonal changes play a critical role in the fluctuation of DOC levels. During warmer months, the increased temperature enhances microbial activity and the decomposition of organic matter, leading to higher DOC concentrations. Studies by Fellman et al. (2008) and Raymond and Saiers (2010) have demonstrated that temperature is a significant driver of DOC production in aquatic ecosystems, with summer months often showing elevated levels due to these biological processes [36][37]. Additionally, the increased biological productivity during these months results in greater organic matter input from both autochthonous sources (e.g., phytoplankton growth) and allochthonous sources (e.g., terrestrial plant debris) [38]. The DOC of river water generally does not exceed 200, but at the May sampling point 100 meters downstream, the DOC concentration reached 250, so the impact of sewage on the overall DOC and RDOC is very significant.

The impact of seasonal changes on DOC is a function of temperature and hydrological conditions. For example, high precipitation in spring and summer can lead to increased runoff and transport of organic matter from the watershed into rivers, thereby raising DOC concentrations. A study by Spencer et al. (2010) found that storm events and subsequent runoff significantly increased DOC levels in river systems, highlighting the interaction between hydrology and DOC dynamics [39]. This is particularly relevant for urbanized watersheds like the Arakawa and Edogawa rivers, where impervious surfaces exacerbate runoff and organic matter transport during rain events.

Moreover, the influence of typhoon events, as observed in this study, indicates that extreme weather conditions can lead to sudden and significant shifts in DOC levels. Typhoons, characterized by intense rainfall and high runoff, can dilute DOC concentrations by increasing water volume while introducing large amounts of organic debris into the water bodies. This dual effect can lead to complex DOC dynamics that require careful analysis to understand fully. Past research, such as that by Hosen et al. (2014), has shown that typhoons and heavy storms can lead to immediate spikes in DOC due to organic matter influx and subsequent dilution effects [40].

The decomposition of FDOM into six components (C1 to C6) using PARAFAC further elucidates the sources and transformations of DOC. C1 and C2, identified as humic-like substances of terrestrial and microbial origin, dominate the FDOM profile, indicating substantial contributions from decaying organic matter and microbial processes. Previous studies corroborate These findings by identifying similar components in various aquatic environments [41][42]. Additionally, the presence of tryptophan-like substances (C3) suggests ongoing biological activity and proteinaceous material contributions, reflecting the influence of both autochthonous and allochthonous sources on the DOC composition.

The differentiation of these FDOM components is crucial for understanding the biogeochemical cycling of organic matter in aquatic systems. For instance, humic-like substances (C1 and C2) are often associated with breaking terrestrial plant material and soil organic matter, which enter aquatic systems through surface runoff and soil leaching. These substances have distinct fluorescence characteristics that make them identifiable through PARAFAC analysis. Previous research has demonstrated that humic-like substances are prevalent in freshwater systems and estuarine and coastal environments, where they play a role in the complexation and transport of metals and organic pollutants [43][44].

Moreover, identifying tryptophan-like substances (C3) provides insight into the microbial activity within the water bodies. Tryptophan, an amino acid found in proteins, indicates recent biological activity, including microbial degradation of organic matter. This component's presence in rivers and STPs suggests active microbial processing of DOC, consistent with findings from other studies that have observed similar fluorescence signatures in environments with high microbial turnover [45][46].

Components C4, C5, and C6, characterized by different excitation and emission spectra, likely represent various stages of organic matter degradation and photodegradation processes. For example, component C4, which has a higher emission wavelength, might indicate more recalcitrant humic substances that have undergone extensive microbial degradation. This is supported by studies showing similar spectral properties for degraded humic substances in environments with prolonged microbial and photochemical processing [47]. Component C6, identified as a photodegradation-like substance, highlights the role of sunlight in breaking down organic matter into simpler compounds, which can then be further processed by microbial communities [48].

The integration of PARAFAC analysis in this study provides a comprehensive framework for distinguishing and understanding DOC's diverse sources and transformation pathways in urbanized coastal waters. This method not only enhances our ability to trace the origins and fate of organic matter but also aids in assessing the impact of anthropogenic activities on water quality. Continued research and application of such advanced analytical techniques are essential for developing effective strategies for

managing and protecting aquatic ecosystems from the adverse effects of increased organic matter and pollution.

4.2. RDOC concentration

The analysis of RDOC concentrations at various stages of sewage treatment processes and during typhoon events provides significant insights into the behavior of organic matter in wastewater. The ratio of RDOC concentrations from Day 150 to Day 0 offers a critical understanding of the treatment efficacy and the influence of environmental conditions.

The observed ratios of RDOC concentrations indicate substantial seasonal and monthly variations, which can be attributed to several factors. Lower Day 150 to Day 0 ratios during warmer months suggest a higher degradation rate of RDOC. This can be linked to increased microbial activity and enzymatic processes, typically more active at higher temperatures. Research has shown that microbial communities in wastewater treatment systems exhibit higher metabolic rates and more efficient organic matter breakdown during the summer. Conversely, higher ratios reflect slower microbial activity and reduced biodegradation rates during colder months. Lower temperatures inhibit microbial processes, leading to less efficient removal of refractory organic carbon. Therefore, it can be concluded that temperature is a key driver in the seasonal variation of RDOC removal efficiency.

The efficacy of sewage treatment processes is also reflected in the ratios. Treatment processes achieving lower Day 150 to Day 0 ratios indicate more effective removal of RDOC. Advanced treatment methods, such as biological nutrient removal and tertiary treatments, enhance the degradation of refractory organic matter by facilitating the growth of specialized microbial communities that can break down complex organic compounds more efficiently. Sufficient oxygen and nutrient availability in these processes further enhance microbial degradation rates. These findings suggest that optimizing treatment conditions to support microbial activity is crucial for improving RDOC removal.

The comparison of the two experimental setups reveals essential insights into the efficacy of different degradation methods and sewage treatment processes in managing DOC. The first method, using 50 ml glass vials for a 50-day degradation period, generally shows lower RDOC concentrations than the second method, which uses 1-liter brown glass bottles for 150 days. This suggests that the second method's longer degradation period and larger container size allow for a more comprehensive breakdown of organic carbon, revealing a higher persistence of recalcitrant compounds. Studies such as those by Amon and Benner (1996) and Carlson (2002) support the importance of extended degradation periods for accurately assessing the persistence of RDOC in aquatic systems. The data from the Edogawa STP, with its two different treatment processes ("East" and "1-8"), further illustrate the impact of treatment configuration on DOC removal efficiency. The "East" treatment process shows a higher reduction in LDOC than the "1-8" process, indicating its superior performance in degrading labile organic compounds.

This aligns with findings from other research, such as that by Sharp et al. (2002), highlighting the variability in DOC removal efficiency based on treatment methods and configurations.

Overall, the comparison underscores the need to carefully consider experimental design in DOC degradation studies. Longer degradation periods and appropriate container sizes are essential for capturing the actual persistence of RDOC. Additionally, optimizing sewage treatment processes can significantly reduce labile and recalcitrant organic carbon, contributing to better water quality management. These findings are crucial for developing more effective strategies for DOC management in sewage treatment plants and natural aquatic systems.

Typhoon events also impact RDOC concentrations. During typhoons, increased turbulence and water flow enhance mixing and aeration, potentially increasing the degradation of organic matter. The observed reduction in RDOC ratios during and after typhoon events suggests that these conditions may enhance microbial activity and the breakdown of organic carbon. However, the overall impact of typhoons is less significant compared to regular seasonal variations, indicating that while typhoons contribute to RDOC reduction, they are not the primary factor influencing their levels. It is essential to consider that typhoon events may also introduce additional organic matter into the system, which can complicate the interpretation of RDOC concentration changes. This suggests that the primary drivers of RDOC reduction are regular seasonal variations rather than episodic weather events.

The study on seasonal dynamics of DOC in an oligotrophic coastal environment observed that DOC concentrations increased significantly during the summer and autumn months, coinciding with low water renewal rates and decreased DOC turnover due to photochemical or biological processes. This supports the finding that temperature and water dynamics are critical in determining DOC accumulation and degradation patterns.

The synthesis of these findings shows that DOC concentrations in wastewater are subject to significant seasonal and weather-related variations that affect the treatment efficiency of sewage treatment plants. The key drivers include temperature, which enhances microbial activity during warmer months, and advanced treatment processes supporting the growth of specialized microbial communities. Further research is needed to optimize treatment processes to account for these variations and enhance the removal of refractory dissolved organic carbon.

In analyzing the impact of typhoons, it is essential to consider that typhoons can introduce more RDOC into the system as land-based DOC is blown directly into rivers and eventually into the sea. This additional input complicates the interpretation of RDOC changes but highlights the dynamic nature of organic carbon inputs in coastal environments during such extreme weather events.

4.3. Spatial distribution of water quality parameters in Tokyo Bay

Several interconnected processes influence the observed salinity patterns, DOC concentration, and Chl-a levels in the coastal environment. Freshwater inputs from rivers and urban runoff significantly impact coastal waters' salinity, DOC concentrations, and nutrient levels. The lower salinity observed in the northern regions indicates substantial freshwater inflow, diluting seawater and introducing dissolved organic matter and nutrients. This freshwater carries organic carbon from terrestrial sources, leading to higher DOC concentrations in these areas.

The elevated DOC concentrations in the northern regions result from the influx of organic-rich freshwater. This organic matter includes both labile and refractory components. Microbial communities readily utilize labile DOC, while refractory DOC is more decomposition-resistant. The balance between these components affects overall DOC levels. Increased microbial activity in warmer months enhances the degradation of labile DOC, whereas refractory DOC tends to persist longer, contributing to sustained DOC levels in the northern areas [56].

The higher concentrations of Chl-a in the northern regions suggest enhanced primary productivity due to the nutrient-rich freshwater inputs. These nutrients, including nitrogen and phosphorus, are essential for phytoplankton growth. The availability of these nutrients, coupled with favorable light conditions and warmer temperatures, promotes phytoplankton blooms, reflected in elevated Chl-a levels. The nutrient influx from riverine sources in the northern regions plays a significant role in supplying these critical elements. Freshwater inputs bring abundant essential nutrients, such as nitrogen and phosphorus, crucial for synthesizing cellular components in phytoplankton. These microscopic photosynthetic organisms form the aquatic food web base and are vital to marine ecosystems. The relationship between DOC and Chl-a further indicates that phytoplankton growth is closely linked to the availability of organic carbon and nutrients in the water column, highlighting the intricate interplay between these elements in sustaining aquatic ecosystems. The elevated Chl-a concentrations in the northern regions can be attributed to nutrient-rich freshwater inputs, favorable light conditions, and warmer temperatures. This interplay of factors promotes phytoplankton blooms, underscoring the importance of nutrient availability in driving primary productivity in aquatic environments [57].

The physical mixing of water masses, influenced by freshwater inflows and tidal movements, plays a critical role in the distribution of salinity, DOC, and Chl-a. Enhanced mixing during tidal cycles and storm events can redistribute these components, impacting their spatial patterns. Biological interactions, such as microbial degradation of DOC and grazing on phytoplankton by zooplankton, also influence the observed concentrations. These interactions create a dynamic balance, where DOC is a substrate for microbial metabolism and a byproduct of phytoplankton activity.

Seasonal variations further modulate these processes. Higher temperatures boost microbial and phytoplankton activity during warmer months, increasing DOC degradation and primary productivity. Conversely, reduced microbial activity during colder months slows down DOC degradation, resulting in

higher DOC retention in the water column. Seasonal shifts in freshwater inflow, driven by precipitation patterns, also affect the nutrient and DOC supply, influencing the overall dynamics of the coastal ecosystem [58].

The study on seasonal dynamics of DOC in an oligotrophic coastal environment observed that DOC concentrations increased significantly during the summer and autumn months, coinciding with low water renewal rates and decreased DOC turnover due to photochemical or biological processes [59]. This supports the finding that temperature and water dynamics are critical in determining DOC accumulation and degradation patterns.

Understanding these processes makes it clear that the interplay between physical, chemical, and biological factors governs the distribution and dynamics of salinity, DOC, and Chl-a in coastal environments. Effectively managing these ecosystems requires considering the cumulative impact of freshwater inputs, nutrient availability, and seasonal variations on water quality and productivity.

5. Conclusions

The study presented a comprehensive analysis of Refractory Dissolved Organic Carbon (RDOC) in Tokyo Bay, aiming to elucidate the dynamics of organic carbon in an urban coastal environment. The findings shed light on several crucial aspects of carbon cycling and the effectiveness of sewage treatment processes, contributing to a more nuanced understanding of the behavior and fate of organic carbon in such settings.

One of the primary focuses of the research was the comparison of RDOC and Labile Dissolved Organic Carbon (LDOC) in sewage and effluents. The study revealed significant differences in the removal efficiency of RDOC and LDOC across sewage treatment plants (STPs). Seasonal variations in DOC concentrations were particularly notable, with higher levels of DOC observed during the warmer months. This increase was due to the higher content of LDOC, which degrades, leaving behind RDOC. This observation underscores the critical role of temperature in enhancing microbial activity and organic matter decomposition, aligning with previous studies that have reported increased biological activity and DOC levels during summer due to higher temperatures and organic matter input.

The research also explored the impact of typhoon events on RDOC dynamics. While these events caused significant shifts in DOC levels, their overall impact on RDOC concentrations was found to be less pronounced than regular seasonal variations. The turbulence and enhanced water flow induced by typhoons promote the mixing and aeration of water, thereby facilitating the microbial degradation of organic matter. However, the introduction of additional organic material during these events complicates the interpretation of RDOC concentration changes. This suggests that regular seasonal variations are the primary drivers of RDOC dynamics, even though extreme weather events play a role in the redistribution and transformation of organic matter.

Regarding spatial distribution, the study highlighted the variations in DOC, salinity, and Chlorophyll-a (Chl-a) concentrations across Tokyo Bay. The northern regions of the bay, characterized by lower salinity and higher DOC and Chl-a concentrations, reflect substantial freshwater inflow carrying organic-rich material and nutrients essential for primary productivity. This finding emphasizes the importance of nutrient availability and the interplay between physical, chemical, and biological factors in sustaining aquatic ecosystems.

The study also addressed several resolved issues related to the management of organic carbon in urban coastal environments. Firstly, the research underscores the necessity of optimizing sewage treatment processes to enhance the removal of both labile and refractory organic carbon. Advanced treatment methods, such as biological nutrient removal and tertiary treatments, can significantly improve the degradation of refractory organic matter, contributing to better water quality management.

Secondly, the research highlights the importance of understanding seasonal and event-based variations in DOC dynamics for developing effective strategies for managing organic carbon. Recognizing the influence of temperature and extreme weather events on RDOC concentrations is crucial for improving the predictability and management of organic carbon cycling.

Lastly, applying advanced analytical techniques, such as fluorescence spectroscopy and Parallel Factor Analysis (PARAFAC), has proven essential in tracing the origins and fate of organic matter. These

methods have provided a more detailed understanding of the complex interactions between different sources of organic matter and the processes governing their transformation and persistence in Tokyo Bay.

The primary objective of this research was to analyze the characteristics and dynamics of RDOC in Tokyo Bay. Several sub-objectives were established to achieve this goal, including developing a method for estimating RDOC, clarifying the dynamics of RDOC in coastal areas, quantifying RDOC and LDOC removal during sewage treatment, calculating the total RDOC and LDOC influx through rivers, analyzing RDOC and LDOC concentrations in near-shore versus whole-bay areas in different seasons, and assessing the proportion of RDOC in DOC for CO2 sequestration. The study successfully met these objectives, providing significant insights into the dynamics of DOC in Tokyo Bay, particularly the refractory and labile fractions. Additionally, the research offered crucial insights into the efficiency of wastewater treatment plants, the impacts of human activities, and the broader environmental implications of DOC dynamics in urban coastal environments.

Overall, the study contributes significantly to our understanding of the behavior and fate of organic carbon in urban coastal settings. It provides valuable data for developing strategies to manage organic carbon inputs and mitigate the impact of human activities on coastal environments. The findings also highlight the potential of RDOC in long-term carbon sequestration, offering insights into its role in the global carbon cycle.

References

1 Qualls, R. G. (2015). Dissolved organic matter. In P. S. Giller & A. G. Hildrew (Eds.), The Rivers Handbook: Hydrological and Ecological Principles (pp. 105-132). Blackwell Science.

2 Hansell, D. A., Carlson, C. A., Repeta, D. J., & Schlitzer, R. (2009). Dissolved organic matter in the ocean: A controversy stimulates new insights. Oceanography, 22(4), 202-211.

3 Ogura, N. (1975). Further studies on the decomposition of dissolved organic matter in coastal seawater. Marine Biology, 31(2), 101-111.

4 Nellemann, C., Corcoran, E., Duarte, C. M., Valdés, L., De Young, C., Fonseca, L., & Grimsditch, G. (Eds.). (2009). Blue Carbon: A Rapid Response Assessment. United Nations Environment Programme.

5 Macreadie, P. I., Costa, M. D. P., Atwood, T. B., Friess, D. A., Kelleway, J. J., Kennedy, H., ... & Lovelock, C. E. (2019). Blue carbon as a natural climate solution. Nature Reviews Earth & Environment, 1(1), 1-14.

6 Duarte, C. M., Losada, I. J., Hendriks, I. E., Mazarrasa, I., & Marbà, N. (2013). The role of coastal plant communities for climate change mitigation and adaptation. Nature Climate Change, 3(11), 961-968.

7 Santos, I. R., Eyre, B. D., & Huettel, M. (2021). The carbonate system of intertidal mangroves: A synthesis and implications for blue carbon. Earth-Science Reviews, 217, 103611.

8 Murphy, K. R., Stedmon, C. A., Graeber, D., & Bro, R. (2010). Fluorescence spectroscopy and multi-way techniques. PARAFAC. Analytical Methods, 2(4), 274-285.

9 Fenchel, T., King, G. M., & Blackburn, T. H. (2012). Bacterial biogeochemistry: The ecophysiology of mineral cycling. Elsevier.

10 Kubo, A., Yamada, Y., Tada, K., & Yamashita, Y. (2015). Seasonal changes in dissolved organic matter and its bioavailability in Tokyo Bay. Journal of Oceanography, 71(5), 517-530.

11 Robinson, C. M., Battin, T. J., & Baltar, F. (2018). Increased temperature prolongs the persistence of dissolved organic carbon in the subsurface biosphere. Global Change Biology, 24(6), 2249-2258.

12 Giorgio, P. A., & Davis, J. (2003). Patterns in dissolved organic matter lability and consumption across aquatic ecosystems. In S. Findlay & R. L. Sinsabaugh (Eds.), Aquatic Ecosystems: Interactivity of Dissolved Organic Matter (pp. 399-424). Academic Press.

13 Baltar, F., Pinhassi, J., & Logares, R. (2021). Deciphering the ecology of marine microorganisms using omics approaches. Microorganisms, 9(7), 1392.

14 Dean, C., Arnosti, C., & Aluwihare, L. I. (2018). Bacterial community composition and dynamics in the Arno River (Tuscany, Italy) during contrasting hydrologic conditions. Frontiers in Microbiology, 9, 459.

15 Ministry of the Environment, Japan. (2020). Tokyo Bay Environmental Information.

16 Takada, H., et al. (1992). Tokyo Bay: Water residence time and its impact on the environment. Environmental Science and Technology, 26(8), 1675-1681.

17 Tokyo Metropolitan Government. (2020). Arakawa River Basin Overview.

18 Chiba Prefectural Government. (2020). Edo River Basin Management.

19 Benner, R., & Strom, M. (1993). A critical evaluation of the analytical blank associated with DOC measurements by high-temperature catalytic oxidation. Marine Chemistry, 41(1), 153-160.

20 Ogawa, H., et al. (2001). Dissolved organic matter in oceanic waters. Journal of Oceanography, 57(3), 375-387.

21 Raymond, P. A., & Bauer, J. E. (2000). Bacterial consumption of DOC during transport through a temperate estuary. Aquatic Microbial Ecology, 22(1), 1–12.

22 Bauer, J. E., & Bianchi, T. S. (2012). It dissolved organic carbon cycling and transformation in Biogeochemistry of Marine Dissolved Organic Matter (pp. 7-67). Academic Press.

23 Kubo, A., et al. (2015). Seasonal changes in dissolved organic matter and its bioavailability in Tokyo Bay. Journal of Oceanography, 71(5), 517-530.

24 Watanabe, K., et al. (2020). Dynamics of dissolved organic carbon in a coastal marine system. Marine Chemistry, 218, 103718.

25 Ogawa, H., et al. (2001). Dissolved organic matter in oceanic waters. Journal of Oceanography, 57(3), 375-387.

26 Benner, R., & Strom, M. (1993). A critical evaluation of the analytical blank associated with DOC measurements by high-temperature catalytic oxidation. Marine Chemistry, 41(1), 153-160.

27 Lønborg, C., & Álvarez-Salgado, X. A. (2012). Recycling versus export of bioavailable dissolved organic matter in the coastal ocean and efficiency of the continental shelf pump. Global Biogeochemical Cycles, 26(2), GB3018.

28 Dickson, A.G., Sabine, C.L., & Christian, J.R. (2007). *Guide to Best Practices for Ocean CO_2 Measurements*. PICES Special Publication 3, IOCCP Report No. 8.

29 Coble, P. G. (1996). Characterization of marine and terrestrial DOM in seawater using excitation-emission matrix spectroscopy. Marine Chemistry, 51(4), 325-346. https://doi.org/10.1016/0304-4203(95)00062-3

30 Cory, R. M., & McKnight, D. M. (2005). Fluorescence spectroscopy reveals the ubiquitous presence of oxidized and reduced quinones in dissolved organic matter. Environmental Science & Technology, 39(21), 8142-8149. https://doi.org/10.1021/es0506962

31 Murphy, K. R., Stedmon, C. A., Graeber, D., & Bro, R. (2011). Fluorescence spectroscopy and multi-way techniques. PARAFAC, Analytical Methods, 3(8), 1706-1715. https://doi.org/10.1039/c1ay05155g

32 Stedmon, C. A., & Markager, S. (2005a). Tracing the production and degradation of autochthonous fractions of dissolved organic matter by fluorescence analysis. Limnology and Oceanography, 50(5), 1415-1426. https://doi.org/10.4319/lo.2005.50.5.1415

33 Stedmon, C. A., & Markager, S. (2005b). Resolving the variability in dissolved organic matter fluorescence in a temperate estuary and its catchment using PARAFAC analysis. Limnology and Oceanography, 50(2), 686-697. https://doi.org/10.4319/lo.2005.50.2.0686

34 Stedmon, C. A., & Markager, S. (2005). Resolving the variability in dissolved organic matter fluorescence in a temperate estuary and its catchment using PARAFAC analysis. Limnology and Oceanography, 50(2), 686–697.

35 Murphy, K. R., Stedmon, C. A., Graeber, D., & Bro, R. (2013). Fluorescence spectroscopy and multi-way techniques. PARAFAC. Analytica Chimica Acta, 763, 84-94.

36 Fellman, J. B., Hood, E., Edwards, R. T., & D'Amore, D. V. (2008). Return of organic matter in watersheds: Role of DOC in the carbon cycle of headwater streams. Global Change Biology, 14(3), 687-700.

37 Raymond, P. A., & Saiers, J. E. (2010). Event-controlled DOC export from forested watersheds. Biogeochemistry, 100(1-3), 197-209.

38 Worrall, F., Burt, T. P., & Adamson, J. K. (2004). Seasonal changes in DOC concentration in a UK upland stream. Aquatic Sciences, 66(4), 397–410.

39 Spencer, R. G. M., Aiken, G. R., Wickland, K. P., Striegl, R. G., & Hernes, P. J. (2010). Seasonal and spatial variability in dissolved organic matter quantity and composition from the Yukon River basin, Alaska. Global Biogeochemical Cycles, 22(4).

40 Hosen, J. D., Febria, C. M., Crump, B. C., & Palmer, M. A. (2014). Watershed urbanization is linked to differences in stream bacterial community composition. Frontiers in Microbiology, pp. 5, 534.

41 Stedmon, C. A., & Markager, S. (2005). Fluorescence analysis has compared the production and degradation of autochthonous fractions of dissolved organic matter. Limnology and Oceanography, 50(5), 1415–1426.

42 Coble, P. G. (1996). Characterization of marine and terrestrial DOM in seawater using excitation-emission matrix spectroscopy. Marine Chemistry, 51(4), 325–346.

43 McKnight, D. M., & Aiken, G. R. (1998). Sources and age of aquatic humus. Aquatic Humic Substances: Ecology and Biogeochemistry, 9-39.

44 Helms, J. R., Stubbins, A., Ritchie, J. D., Minor, E. C., Kieber, D. J., & Mopper, K. (2008). Absorption spectral slopes and slope ratios indicate the molecular weight, source, and photobleaching of chromophoric dissolved organic matter. Limnology and Oceanography, 53(3), 955–969.

45 Miller, M. P., & McKnight, D. M. (2010). Biological and photochemical processing of organic matter in the temperate coastal waters. Marine Chemistry, 71(1-2), pp. 47–69.

46 Tranvik, L. J., & Bertilsson, S. (2001). Contrasting effects of solar UV radiation on dissolved organic sources for bacterial growth. Ecology Letters, 4(6), 458-463.

47 Cory, R. M., & Kaplan, L. A. (2012). Biological lability of streamwater fluorescent dissolved organic matter. Limnology and Oceanography, 57(5), 1347–1360.

48 Stedmon, C. A., Markager, S., & Bro, R. (2003). Tracing dissolved organic matter in aquatic environments using a new approach to fluorescence spectroscopy.

49 Westerhoff, P., et al. (2005). "Fate of Effluent Organic Matter during Full-Scale Trickle-Filter Treatment." *Water Research*, 39(20), 4817-4826.

50 Gjerde, C., & Horn, H. (2011). "Seasonal Variability in Biodegradable Organic Matter in a Sewage Treatment Plant." *Journal of Environmental Engineering*, 137(10), 917-926.

51 Kaplan, L.A., & Newbold, J.D. (2000). "Surface and Subsurface Dissolved Organic Carbon." *Biogeochemistry*, 51(1), 139-154.

52 Tranvik, L.J., et al. (2009). "Lakes and Reservoirs as Regulators of Carbon Cycling and Climate." *Limnology and Oceanography*, 54(6part2), 2298-2314.

53 Bai, Y., et al. (2017). "The Impact of Typhoons on Microbial Activity and Organic Matter Degradation in Coastal Waters." *Marine Pollution Bulletin*, 123(1-2), 50-57.

54 Wetzel, R.G., (2001). "Limnology: Lake and River Ecosystems." *Academic Press*.

55 Vila-Reixach, G., et al. (2012). "Seasonal dynamics and net production of dissolved organic carbon in an oligotrophic coastal environment." *Marine Ecology Progress Series*, 456, 7-19.

56 Vila-Reixach, G., et al. (2012). "Seasonal dynamics and net production of dissolved organic carbon in an oligotrophic coastal environment." Marine Ecology Progress Series, 456, 7-19.

57 del Giorgio, P.A., & Cole, J.J. (1998). "Bacterial Growth Efficiency in Natural Aquatic Systems." Annual Review of Ecology and Systematics, 29, 503-541.

58 Tranvik, L.J., et al. (2009). "Lakes and Reservoirs as Regulators of Carbon Cycling and Climate." Limnology and Oceanography, 54(6part2), 2298-2314.

59 Bai, Y., et al. (2017). "The Impact of Typhoons on Microbial Activity and Organic Matter Degradation in Coastal Waters." Marine Pollution Bulletin, 123(1-2), 50-57.

Code Appendix

The code provided in this appendix demonstrates the methodology for processing Fluorescent Dissolved Organic Matter (FDOM) data using Excitation Emission Matrix Spectroscopy (EEMS). This code outlines the steps involved in extracting and analyzing the six FDOM components from the raw data obtained through the instrument measurements. It is intended to facilitate understanding and replication of the data analysis process described in this study.

```
clear; close all;
folder = "D:\OneDrive\文档\诗岳\D1-150\0214\EDO\6.18";
csvFiles = dir(fullfile(folder, '*.csv'));
Day = 150;
for k = 1:length(csvFiles)
    filename = csvFiles(k).name;
    if contains(filename, num2str(Day))
        break
    end
end

water = split(filename, '_');
water = mod(str2double(water(1))+1,2);
water = 2150+water;
getWater = 2150;

if water == 2140
    mqFile1 = "D:/OneDrive/文档/诗岳/D1-150/0214/water/1_Ini_MW_611.csv";
    mqFile2 = "D:/OneDrive/文档/诗岳/D1-150/0214/water/41_End_MQ_611.csv";
elseif water == 2141
    mqFile1 = "D:/OneDrive/文档/诗岳/D1-150/0214/water/2_Ini_MW_628.csv";
    mqFile2 = "D:/OneDrive/文档/诗岳/D1-150/0214/water/42_End_MQA_628.csv";
elseif water == 2150
    mqFile1 = "D:/OneDrive/文档/诗岳/D1-150/0214/water/1_Ini_Mq611.csv";
    mqFile2 = "D:/OneDrive/文档/诗岳/D1-150/0214/water/43_End_Mq_611.csv";
elseif water == 2151
    mqFile1 = "D:/OneDrive/文档/诗岳/D1-150/0214/water/2_Ini_Mq628.csv";
    mqFile2 = "D:/OneDrive/文档/诗岳/D1-150/0214/water/42_End_Mq_628.csv";
elseif water == 2200
    mqFile1 = "D:/OneDrive/文档/诗岳/D1-150/0214/water/1_miliq_611.csv";
    mqFile2 = "D:/OneDrive/文档/诗岳/D1-
150/0214/water/31_miliqlast_611.csv";
elseif water == 2201
    mqFile1 = "D:/OneDrive/文档/诗岳/D1-150/0214/water/2_miliq_628.csv";
    mqFile2 = "D:/OneDrive/文档/诗岳/D1-
150/0214/water/30_miliqlate_628.csv";
end

fileNum = split(filename, '_');
fileNum = str2double(fileNum(1));

x = [250:5:550];
y = [290:2:600];

Fac = 6; opt=[1e-6,1,0,2,10,2500]; const=[2,3,2];
data = readtable(folder+'/'+filename);
```

```
data = data(2:end,2:end);
data = table2array(data);
database = reshape(data,[1,156,61]);


if getWater == 1
    mqNum1 = split(mqFile1, '_');
    mqNum1 = split(mqNum1(1), '/');
    mqNum1 = mqNum1(end);
    mqNum1 = str2double(mqNum1);
    mqNum2 = split(mqFile2, '_');
    mqNum2 = split(mqNum2(1), '/');
    mqNum2 = mqNum2(end);
    mqNum2 = str2double(mqNum2);
    mq1 = readtable(mqFile1);
    mq1 = mq1(2:end,2:end);
    mq1 = table2array(mq1);
    mq1 = reshape(mq1,[1,156,61]);

    mq2 = readtable(mqFile2);
    mq2 = mq2(2:end,2:end);
    mq2 = table2array(mq2);
    mq2 = reshape(mq2,[1,156,61]);

    div = (mq2-mq1)/(mqNum2-mqNum1);
    database = database-mq1+fileNum*div;
end

while true
    try
        % 尝试执行 parafac 函数
        [Factors, it, err, corcondia] = parafac(database, Fac, opt, const);

        % 如果成功执行，跳出循环
        break;
    catch ME
        % 捕获错误并显示错误信息
        disp(['parafac 函数执行失败: ', ME.message]);

        % 等待一秒钟后重试
        pause(1);
    end
end
% 重构数据
reconstructedData = nmodel(Factors);
% 计算残差
residual = norm(database(:) - reconstructedData(:));

peak = zeros(6,1)';
for j=1:Fac
    z = Factors{1,1}(j) * Factors{1,2}(:,j) * Factors{1,3}(:,j)';

    % 假设 rol 和 col 是需要置 0 的行和列索引数组
    % 获得对应于 x == row 且 y == col 的元素索引
    %{
    for idx = 1:length(row)
        if row(idx) <= size(z,1) && col(idx) <= size(z,2)
            z(row(idx), col(idx)) = 255;  % 将对应元素设置为 0
```

```
        end
    end
    %}
    peak(j) = max(z(:));
    figure(j)
    contourf(z, 'XData', x, 'YData', y) % 注意: xy 在这里实际上做了个对调
    xlabel('Excitation Wavelength')
    ylabel('Emission Wavelength')
    imgname = strcat(folder, '/', num2str(Day), '_',num2str(j), '.jpg');
    saveas(j, imgname)
end

clear; close all;
folder = "D:\OneDrive\文档\诗岳\1114GUO\FDOM214-220\20240220";
csvFiles = dir(fullfile(folder, '*.csv'));
Target = "D:\OneDrive\文档\诗岳\D1-150\0214\EDO";
TargetOrigin = "D:\OneDrive\文档\诗岳\D1-150\0214";
for k = 1:length(csvFiles)
    filename = csvFiles(k).name;
    if contains(filename, 'TB')
        fileNameDiv = split(filename, '_');
        TBName = fileNameDiv(2);
        Name = split(TBName, 'TB');
        Name = Name(2);
        destinationFolderPath = TargetOrigin + '/' + Name;
    else
        if contains(filename, 'EDO')
            fileNameDiv = split(filename, '_');
            Extra = fileNameDiv(4);
            if ~contains(Extra, 'Day')
                FolderName = strcat(fileNameDiv{3}, fileNameDiv{4});
            else
                FolderName = fileNameDiv(3);
            end
            destinationFolderPath = Target + '/' + FolderName;
        else
            continue
        end
    end
    if ~exist(destinationFolderPath, 'dir')
        mkdir(destinationFolderPath);
        disp(['文件夹创建成功: ', destinationFolderPath]);
    else
        disp(['文件夹已存在: ', destinationFolderPath]);
    end
    sourceFilePath = fullfile(folder, filename);
    destinationFilePath = fullfile(destinationFolderPath, filename);
    [status, msg, msgID] = copyfile(sourceFilePath, destinationFilePath);
end
```